STRESS AND RELIABILITY OF HIGH-POWER GaAs-BASED LASERS

BONDING STRESS AND RELIABILITY OF HIGH-POWER GaAs-BASED LASERS

By

DUBRAVKA LISAK, B.Eng.Society

A Thesis

Submitted to the School of Graduate Studies

in Partial Fulfilment of the Requirements

for the Degree

Master of Engineering

McMaster University

MASTER OF ENGINEERING (1999) McMaster University
(Engineering Physics) Hamilton, Ontario

TITLE: Bonding Stress and Reliability of High-Power GaAs-Based Lasers.

AUTHOR: Dubravka Lisak, B.Eng.Society (McMaster University)

SUPERVISOR: Professor D. T. Cassidy

NUMBER OF PAGES: viii, 72

Abstract

This thesis documents a study of bonding stress and the reliability of GaAs-based lasers for high-power applications. GaAs-based lasers were bonded to oxygen-free high-conductivity (OFHC) copper heat sinks using a eutectic PbSn solder or a silver-filled conductive epoxy, and life tested. Epoxy-bonded devices were observed to have a larger failure rate on life test than solder-bonded devices. Bonding stress, as measured by the degree of polarization (DOP) of photoluminescence, was found to be the largest in epoxy-bonded devices. As well, the type of heat sink and bonding adhesive affected the stress in the laser material, with bonding stress increasing when there was a larger mismatch of coefficients of thermal expansion between the laser material, adhesive and heat sink.

The reliability of the lasers was affected by the amount of force applied to unbonded laser chips. As the applied force increased on a chip centred on a groove, the rate of degradation in the output power increased. A limit in stress tolerance was observed in the lasers, which meant that larger amounts of stress would lead to increased rates of degradation in the output power. As well, the performance of lasers selected from a batch showing poor reliability degraded at an accelerated rate after several hours of operation under applied strain.

Acknowledgments

I would like to thank many people who have helped me during my Master's studies. Dr. Cassidy has extended his wisdom in teaching me useful research skills and I thank him for the helpful conversations and supervision. I would also like to thank Alan Moore and all of the people at EG&G Optoelectronics in Vaudreuil who helped me flex my engineering muscles in an industrial laboratory.

My family deserves an enormous round of thanks. My parents, Stjepan and Štefica Lisak, my grandparents, Josip and Rosa Golub and my brother Darko and his wife Barbara have helped me through many difficult times and I am very grateful for their patience.

Matthew Pearson has been an important person in my academic and personal life. His encouragement has given me the strength to tackle the greatest challenges, and his thoughtfulness has been invaluable to me.

Lastly, my friends in and around school have made day-to-day life fun and rewarding. Thanks to Fran and Ann in the office, and Paul Colbourne, and thanks to

Irene, Bridget, SuMei, Doug, Luke, Sam, Chris, Adam, Ted, John, Mike and the whole gang. You are the best.

Table of Contents

List of Figures

List of Tables

Chapter 1 Introduction

Research into the reliability of semiconductor diode lasers has been vast. Laser degradation and poor reliability have been related to facet oxidization leading to catastrophic optical damage (COD) and to the presence of pre-existing defects within the laser material [1,2]. However, the effect of mechanical stress on the reliability of semiconductor lasers has also been a subject of recent research. This report discusses effects of bonding stress on high-power GaAs-based lasers. In this chapter, an overview of areas of research into stress in semiconductors is presented, with emphasis on measurements of degree of polarization (DOP).

1.1 Stress in Semiconductor Diode Lasers

Mechanical stress is a concern in the design and manufacture of semiconductor diode lasers. Stress has been shown to affect threshold current, the emission wavelength and the polarization of laser light [3]. Studies have also shown that stress may significantly reduce the lifetime of lasers [4-6]. Work in this field has shown that stress can result from factors such as the external application of force onto a laser, oxide layers, metallization, lattice mismatch, bonding and packaging, or die attachment, which is a focus in this project [7-13]. The work presented in this thesis deals with bonding stress

and effects of stress on high-power GaAs-based diode lasers. The results of this project offer useful information on effects of die attachment on the reliability of these lasers.

To observe effects of bonding stress and general stresses in GaAs-based lasers, a technique known as the degree of polarization (DOP) of photoluminescence was used [8]. This technique evaluates stress through measurements of resolved polarization signals. DOP is defined as

$$DOP = \frac{L_x - L_y}{L_x + L_y} \tag{1}$$

where L_x and L_y are the measured polarization components of light along the horizontal and vertical directions, respectively. If the two measured polarization components have equal intensities, the corresponding DOP value would be zero. DOP measurements have been shown to have a spatial resolution of approximately 1 μm and a strain resolution of 10^{-5} [8].

Experiments have shown a relationship between the DOP measured from photoluminescence of a III-V semiconductor and the mechanical stresses σ_{xx}-σ_{yy} in the semiconductor as

$$DOP = K_\sigma(\sigma_{xx} - \sigma_{yy}) \tag{2}$$

where the terms in parentheses describe the local stress in the region emitting the

photoluminescence [8]. This relation is discussed in more detail in the following chapters.

Other techniques have been employed to measure mechanical stresses in semiconductor devices. One common method is X-ray diffraction, which observes X-ray diffraction pattern shifts from strained semiconductors [10,13]. However, this technique obtains topographic information of an entire surface which does not provide as high a resolution as DOP does, and a sample area of the order of $1cm^2$ or more is required for such measurements. Another technique is the observation of birefringence through an IR microscope [14], which is only used as a qualitative technique to study stress. Fourier transform photocurrent measurements have also been used. In this case, a diode laser is used as a photodetector, and the front facet is illuminated to provide a signal that is fed to a spectrometer, which provides information on stress in the active layer. This technique is limited because the semiconductor sample studied must be a laser, and the reported spatial resolution is around 200 μm [15]. Degree of polarization is a useful method to determine detailed stress patterns in bulk III-V semiconductors or devices fabricated with those materials and this method has been useful for the analysis of bonding effects on lasers.

1.2 Bonding Adhesives

There are two types of bonding adhesives that have been studied in this project, both of which are common in packaging of semiconductor lasers. Solder has been the bonding adhesive of choice for diode lasers for many years. Recently, however, conductive epoxies have become significant alternatives, and are now considered for many electronic components, not only for packaging of diode lasers. Results obtained in this project demonstrate that a bonding adhesive plays an important role in the performance of diode lasers. The following is a brief description of the two types of bonding adhesives used in the experiments for this report, and will outline the differences in the materials and techniques that may affect the device significantly.

Solders have been standard bonding adhesives for lasers. Common practice in bonding using solders has been to heat the solder to the temperature at which it melts. In the case of eutectic PbSn solder, this temperature is approximately 200°C. The laser chip is placed over the heat sink such that, when the solder is placed between the chip and the heat sink, a metallurgical reaction occurs, forming a solid bond between the materials. During this process, solder flux is used primarily to prevent the metals from oxidizing and to maintain clean surfaces on the materials being soldered together. However, in many cases, the flux is a corrosive material which can eventually destroy the laser and heat sink materials. Clearly, it is important to ensure that the assembled device is cleaned

properly.

Alternatively, conductive epoxies have gained use as bonding adhesives for many electronic components, including diode lasers. Possibly one of the most important driving forces behind this technology has been the need to reduce contamination of the environment. Not only does the solder flux pose serious threats to diode lasers if not cleaned properly, the lead content in many of the devices needs to be reduced or eliminated, since PbSn solder has been a common adhesive.

An epoxy is a polymer which has the ability to adhere to materials after it has cured. For the applications requiring an electrically conductive adhesive, epoxy is filled with metal particles such as silver, copper, nickel or metal alloys such as SnBi [16, 19]. In its initial state, epoxy is generally a viscous liquid. When bonding a diode laser, this liquid is dispensed from a syringe to an area on the heat sink, and the laser chip is then placed on the epoxy. To complete the bonding process, the epoxy is cured at a specified temperature during a specified time such that the epoxy becomes a fixed material which holds the laser chip securely to the heat sink.

As the technology of conductive epoxies becomes more wide-spread in the electronics industry as well as others, it is important to develop these conductive

adhesives such that they meet, or surpass, the specifications of their solder counterparts with respect to mechanical, thermal and electrical properties. Studies have shown that some conductive epoxies exhibit higher volume resistivity, lower adhesion strength and lower reliability than PbSn solder [16-18], particularly silver-filled epoxies. As well, the workability of epoxies is difficult because, once they are cured, their properties cannot be reversed. However, solders can be heated to temperatures below melting temperatures, giving soft adhesives for reworking. On the other hand, some conductive epoxies have demonstrated improved performance in conductivity and reliability with treated surfaces, more control of layer thickness, and low amounts of conductive filler [16, 18]. As techniques have improved with regards to bonding processes, interest has grown to replace solders with conductive epoxies.

1.3 New Contributions

The experimental work in this project has been divided into two segments. In the first segment, the effect of bonding on high-power GaAs-based lasers has been investigated. Degree of polarization was measured from the photoluminescence at the front facet of GaAs-based lasers bonded to different heat sinks. Lasers exhibited lower stress at the facet when bonded to heat sinks with coefficients of thermal expansion (CTE) that were closest to that of the laser material. As well, effects of bonding adhesives with CTE values significantly larger than the laser material were also evident.

In the second segment of this work, the general effect of stress on high-power GaAs-based lasers was studied. Observations of optical output power of lasers showed an increase in the rate of degradation with increased applied stress. This was achieved by mounting an unbonded GaAs-based laser chip on a groove in a copper plate and applying various forces to the chip while driving current through the laser. The rate of degradation of a standard laser was directly related to the applied force, while a laser from a poor batch exhibited accelerated degradation after several hours of operation.

1.4 Summary

Results presented in this report provide useful insight into processes that may affect laser reliability. Bonding stress measurements have been integral in the packaging design of high-power GaAs-based lasers at EG&G Canada. The technique relating applied stress to degradation rates for unbonded lasers functions as a useful tool to characterize laser batches. This information is also beneficial to industries which manufacture other semiconductor devices.

This thesis is divided into seven chapters. This chapter serves as a brief description of the significance of this work on die attachment of semiconductor diode lasers. Chapter 2 provides an overview of the theory that relates stress on a crystal lattice to the polarization of photoluminescence of crystals such as GaAs. The bonding process of high-power GaAs-based diode lasers is investigated in Chapter 3. In Chapter 4, the

effect of applied force on unmounted GaAs-based laser chips is studied on the resulting stress in the lasers and the degradation rate of the operating laser. Major conclusions from the experiments in this thesis are discussed in Chapter 5. Suggestions for further research are outlined in Chapter 6, and references cited in this thesis are listed in the final chapter.

Chapter 2 Background

2.1 Introduction

A pure, unstrained crystal such as GaAs or InP exhibits symmetry in the lattice. However, if a uniaxial strain is introduced to the crystal, the atomic arrangement of the lattice is altered, which causes a change in the energy band structure of the crystal. This ultimately affects the luminescence of the crystal because the probability of transitions between the conduction and valence bands for a crystal under zero strain is different from the probability of transitions in a crystal under a uniaxial strain. Luminescence can provide information on the amount of strain induced in a semiconductor.

To explain the changes that occur in a semiconductor diode laser such that its operating characteristics are altered, this section includes a brief discussion that provides a background on the effect of strain on the band structure of III-V semiconductor crystals. The changes that occur in the photoluminescence of these materials as a result of strain on band structure are also approximated and related to the degree of polarization.

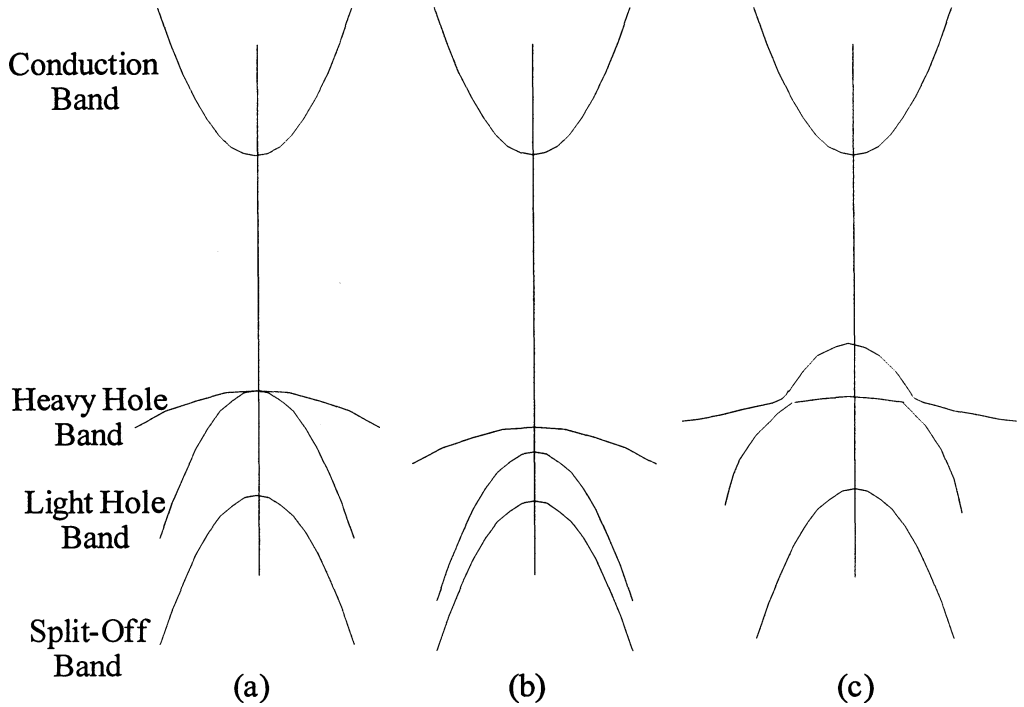

Figure 2.1 Schematic of E-k curves of a III-V semiconductor along the k-axis that is parallel to the axis of the strain.

2.2 Stress-Induced Changes in Band Structure

When a uniaxial stress is applied to a crystal, the symmetry in the crystal is altered. This causes a deformation in the energy bands. Depending on whether the stress is compressive or tensile, the energy spacing between the heavy hole bands and the light hole bands will be affected. A basic illustration of the effects is presented in Figure 2.1. The diagram shows the *E-k* curve for a typical III-V semiconductor crystal in the first Brillouin Zone. For an unstrained crystal, one can expect a high degree of isotropy in

which the energy bands are the same along the x, y and z directions, which is directly related to the degree of symmetry in the atomic arrangement of the crystal lattice (Figure 2.1 (a)). However, if a uniaxial tensile strain is introduced on a crystal along the y axis, for example, then the symmetry in the lattice structure is affected, and the heavy hole and light hole bands split, with the energy spacing between the bands depending on the amount of stress applied in the y direction (Figure 2.1 (b)) [19]. In contrast, a compressive strain along the y axis causes the heavy hole band and light hole band to mix, and the energy separation from the conduction band is reduced (Figure 2.1 (c)).

The changes that occur within the band structure of a crystal can be described in an analytical manner. As mentioned before, when an isotropic crystal is unstrained, the *E-k* curves in the x, y and z directions are identical. It has been shown that, away from k=0, the change in band energy along the y direction is proportional to the strain in that direction, while the *E-k* curves corresponding to the x and z directions remain unchanged. For energy shifts that are much smaller than kT (where k is the Boltzmann constant and T is temperature in Kelvin) most of the holes in the valence bands available for transitions are away from the Brillouin zone center. The change in band energy can be approximated away from k=0 as [19]

$$\Delta E = a\Delta \pm \frac{bB}{2D}\sum_i 3\left(\frac{k_i^2}{k^2}-1\right)\varepsilon_{ii} \qquad (1)$$

where

$$D = \sqrt{B^2 + \frac{C^2}{5}}$$

$$k = \sqrt{k_x^{\,2} + k_y^{\,2} + k_z^{\,2}}$$

and b is the deformation potential of the valence band, B, and C are parameters that characterize the valence band, and i can be coordinate axis x, y or z. The plus and minus signs correspond to the heavy hole and light hole bands, respectively. The term $a\Delta$ refers to the displacement in energy of the entire band. For the purposes of this work, the changes that occur in the band structure are of interest. Thus, considering the changes, (1) can be simplified to [20]

$$\Delta E = \pm \frac{3bB}{2D} \sum_i \frac{k_i^{\,2}}{k^2} \varepsilon_{ii} = \pm \frac{3bB}{2D} \sum_i \varepsilon_{ii} \cos^2 \beta_i \qquad (2)$$

where β_i is the angle between the axis i and the electron momentum vector, **k**. In addition to this shift in energy, other energy shifts take place that are independent of **k** or depend on the magnitude of k but are independent of its direction. These changes do not relate to the degree of polarization of luminescence and are not included in this discussion. It is worth noting that the approximation presented here is valid only for higher temperatures (i.e., room temperature). At low temperatures, this expression is no longer valid. In the work for this project, however, all measurements were obtained at room temperature. Thus, the approximation given here can be assumed for all measurements.

Since a uniaxial strain applied to a crystal alters its band structure, the probability of transitions between conduction and valence bands are also changed. Consequently, luminescence from a crystal structure such as GaAs is also altered. Given this, the changes in polarization states of luminescence can be related to the strain applied to a III-V semiconductor crystal.

To obtain the relation between stress and the polarization states of luminescence, the probability of a transition from the conduction band to the valence band must be determined. This is obtained from the rate of transition from the conduction band to the valence band when photons interact with the crystal. An approximate expression for this rate of transition is given by [22]

$$W_{eh} = \frac{2\pi}{\hbar}|H'_{eh}|^2 \tag{3}$$

where $\hbar$ is Planck's constant and

$$|H'_{eh}|^2 = \left(\frac{eA_o}{2m_o}\right)^2 |M_T|^2 \tag{4}$$

where m_o is the effective mass of a particular valence band, e is the electronic charge of an electron and A_o is proportional to the intensity of the incident radiation. The final parameter to define is the transition matrix element, $|M_T|^2$, which essentially determines the probability of a transition. The transition matrix element is defined as [22]

$$\left|M_T\right|^2 = \left|\left\langle u_1 \left| \mathbf{e}\cdot\mathbf{p} \right| u_2 \right\rangle\right|^2 \tag{5}$$

where u_1 and u_2 are the initial and final states of a particular wave function, respectively. The vector **e** is the unit vector of polarization for incident radiation and **p** is the electron momentum operator. The Bloch functions describing the valence bands of an unstrained crystal can be expressed as linear combinations of the basis functions, u_x, u_y and u_z. If the electron momentum vector was directed along the z axis, then the Bloch functions for such a calculation would be of the following form [22]

$$\begin{aligned}
u_{hh} &= -\tfrac{1}{\sqrt{2}}(u_x + iu_y) & u'_{hh} &= \tfrac{1}{\sqrt{2}}(u'_x - iu'_y) \\
u_{lh} &= \tfrac{1}{\sqrt{6}}(2u_z - (u_x + iu_y)) & u'_{lh} &= \tfrac{1}{\sqrt{6}}(2u'_z - u_x - iu_y) \\
u_{so} &= -\tfrac{1}{\sqrt{3}}(u'_x + iu'_y + u_z) & u'_{so} &= \tfrac{1}{\sqrt{3}}(u_x - iu_y - u'_z)
\end{aligned} \tag{6}$$

where the subscripts hh, lh and so refer to the conduction, heavy hole, light hole bands and split-off respectively. The Bloch function for the conduction band is generally denoted by u_s, where the subscript s symbolizes a similarity to the wave function of the s-orbital of an atom, and u and u′ indicate spin up and spin down functions, respectively. Useful relations which account for symmetry in the Bloch functions are [22]

$$\begin{aligned}
&\left\langle u_s \left| p_i \right| u_j \right\rangle = 0 \quad \text{for i} \neq \text{j} \\
&\left\langle u_s \left| \mathbf{p} \right| u_i \right\rangle = \left\langle u_s \left| p_i \right| u_i \right\rangle = M \\
&\left\langle u_s \left| \mathbf{p} \right| \overline{u}_i \right\rangle = 0
\end{aligned} \tag{7}$$

where M is known as the basis function momentum matrix element. The probability determined considers the relations of symmetry and spin degeneracies. Thus, for an incident electric field, the separate transition matrix elements would be calculated using equations (6) and (7) to give [22]

$$
\begin{aligned}
|M_T|^2_{hh} &= |M|^2 (e_x^2 + e_y^2) \\
|M_T|^2_{lh} &= \tfrac{1}{3}|M|^2 (e_x^2 + e_y^2 + 4e_z^2) \\
|M_T|^2_{so} &= \tfrac{2}{3}|M|^2
\end{aligned}
\tag{8}
$$

These equations can be simplified if the substitution $e_x^2 + e_y^2 = 1 - e_z^2$ is used, since the vector **e** is a unit vector. The term e_z represents a component of the polarization vector that is parallel to the electron **k** vector, which has been defined in this discussion to be directed along the z axis. Thus, the transition matrix elements for the heavy hole band and the light hole band, respectively, are [22]

$$
\begin{aligned}
|M_T|^2_{hh} &= |M|^2 (1 - \cos^2 \alpha) \\
|M_T|^2_{lh} &= |M|^2 (\tfrac{1}{3} + \cos^2 \alpha)
\end{aligned}
\tag{9}
$$

where α is the angle between the electric field vector **e** and the electron momentum vector **k**. These expressions relate $|M|^2$, the probability of a transition from u_c and the basis functions, u_x, u_y and u_z, to $|M_T|^2$, the probability of a transition between u_c and the valence bands, assuming certainty of a state initially being occupied in the conduction band and a state initially being empty in a valence band. The expressions presented here have been

determined using the Bloch functions for an unstrained crystal. However, the probability of a transition can be approximated using these Bloch functions. It is important to note that absolute energy of the split off band is significantly larger than the heavy hole and light hole bands. Thus, the effect of strain on the heavy hole and light hole bands is of greater interest for the remainder of this section.

The preceding discussion considered the probability of one transition occurring between the conduction and valence band, given the certainty of a state being occupied in the conduction band, and a vacancy in a valence band. The total luminescent intensity as a result of all transitions would be estimated by integrating the product of hole densities, electron densities and the transition matrix element over all possible k values. Assuming the transition matrix element varies only slightly for an applied strain, the resulting integral has the form [20]

$$L_{total} = \int |M_T|^2(k) f_e(E_e(k)) f_h(E_h(k) + \Delta E_h(k)) dk \qquad (10)$$

and, converting to spherical coordinates, the integral becomes [20]

$$L_{total} = \int |M_T|^2(\phi,\theta) f_e(E_e(r)) f_h(E_h(r) + \Delta E_h(\phi,\theta)) r^2 \sin\theta dr d\theta d\phi \qquad (11)$$

where $f_e(E_e)$ and $f_h(E_h)$ are the energy dependent Fermi-Dirac distributions of electrons and holes, respectively, and are defined as

$$f_e(E_e) = \frac{1}{\exp[(E_e - E_{fe})/kT + 1]}$$
$$f_h(E_h) = \frac{1}{\exp[(E_{fh} - E_h)/kT + 1]} \quad (12)$$

where E_{fe} and E_{fh} are the quasi-Fermi levels for electrons and holes, respectively, and kT is the product of Boltzmann's constant and temperature in Kelvin. It should be noted that $E_e(r)$ and $E_h(r)$ represent the spherical constant energy surfaces for electrons and holes, respectively, with no applied stress, and $\Delta E_h(\theta,\phi)$ represents the change in hole energy as a result of applied strain. If the material is not heavily p-doped, the assumption E_{fh}-E_h >> kT is valid, and the following simplification can be made [20]

$$f_h(E_h) \approx \exp\left[\frac{E_h - E_{fh}}{kT}\right] \quad (13)$$

Furthermore, $f_h(E_h + \Delta E_h) \approx f_h(E_h)(1+\Delta E_h/kT)$. The expression for total luminescence is now

$$L_{total} = \int f_e(E_e(r)) f_h(E_h(r)) r^2 dr \int |M_T|^2(\theta,\phi)\left[1 + \frac{\Delta E_h(\theta,\phi)}{kT}\right] d\Omega \quad (14)$$

where $d\Omega$ is the differential of a solid angle. The integral can be separated to evaluate the luminescence resulting from the transitions with the heavy hole band and the light hole band. For a uniaxial strain along the x axis, the effect on the valence bands is only along one axis. Considering polarization along the direction of the strain, $\beta_x=\alpha$ and the emitted luminescence becomes [20]

$$L_{hh\|} = \int f_e(E_e(r)) f_h(E_h(r)) r^2 dr \int |M_T|^2_{hh} \left[1 + \frac{3bB\varepsilon}{2DkT} \cos^2 \alpha \right] d\Omega$$
$$= G_{hh} \int (1 - \cos^2 \alpha) \left[1 + \frac{3bB\varepsilon}{2DkT} \cos^2 \alpha \right] d\Omega \quad (15)$$

and

$$L_{lh\|} = \int f_e(E_e(r)) f_h(E_h(r)) r^2 dr \int |M_T|^2_{lh} \left[1 - \frac{3bB\varepsilon}{2DkT} \cos^2 \alpha \right] d\Omega$$
$$= G_{lh} \int (\tfrac{1}{3} + \cos^2 \alpha) \left[1 - \frac{3bB\varepsilon}{2DkT} \cos^2 \alpha \right] d\Omega \quad (16)$$

where $L_{hh\|}$ and $L_{lh\|}$ are the polarizations parallel to the direction of strain for the heavy holes and the light holes, respectively. In this case, β is the angle between **k** and the polarization vector, which is along the strain axis, resulting in $\beta=\alpha$. For a uniaxial strain applied along the y axis, the polarization along the y axis is affected. The expressions for luminescence become [20]

$$L_{hh\perp} = G_{hh} \int (1 - \cos^2 \alpha) \left[1 + \frac{3bB\varepsilon}{2DkT} \cos^2 \beta \right] d\Omega$$
$$L_{lh\perp} = G_{lh} \int (\tfrac{1}{3} + \cos^2 \alpha) \left[1 - \frac{3bB\varepsilon}{2DkT} \cos^2 \beta \right] d\Omega \quad (17)$$

The expressions are quoted to be perpendicular with respect to the x axis. In this case, $\beta \neq \alpha$, because the polarization vector is perpendicular to the axis of reference.

The degree of polarization is defined as

$$\rho = \frac{L_{\parallel} - L_{\perp}}{L_{\parallel} + L_{\perp}} \tag{18}$$

The parameters in this equation can be substituted by adding the luminescences for the heavy hole and light hole bands. Thus, the difference between the polarizations is given by

$$\begin{aligned} L_{\parallel} - L_{\perp} &= L_{\parallel hh} + L_{\parallel lh} - L_{\perp hh} - L_{\perp lh} \\ &= -\frac{3bB\varepsilon_{xx}}{2DkT}(G_{hh} + G_{lh}) \int (\cos^4 \alpha - \cos^2 \alpha \cos^2 \beta) d\Omega \end{aligned} \tag{19}$$

This expression can be simplified by defining an angle, γ, that is between **k** and a vector **c** that is perpendicular to the direction of strain and the perpendicular polarization. Now the direction of strain, the polarization direction and **c** are mutually orthogonal, making $\cos^2\alpha + \cos^2\beta + \cos^2\gamma = 1$. The integral can be simplified to [20]

$$\begin{aligned} \int \cos^2 \alpha \cos^2 \beta d\Omega &= \int \cos^2 \alpha \cos^2 \gamma d\Omega \\ &= \int (\cos^2 \alpha (1 - \cos^2 \alpha - \cos^2 \beta) d\Omega \\ &= \int (\cos^2 \alpha - \cos^4 \alpha - \cos^2 \alpha \cos^2 \beta) d\Omega \\ &= \tfrac{1}{2} \int (\cos^2 \alpha - \cos^4 \alpha) d\Omega \end{aligned} \tag{20}$$

Now, the numerator in the definition of degree of polarization can be written as [20]

$$L_{\parallel} - L_{\perp} = -\frac{3bB\varepsilon_{xx}}{2DkT}(G_{hh} + G_{lh})\int(\tfrac{3}{2}\cos^4\alpha - \tfrac{1}{2}\cos^2\alpha)d\Omega$$
$$= -\frac{4\pi bB\varepsilon_{xx}}{5DkT}(G_{hh} + G_{lh}) \qquad (21)$$

If the assumption is made that $3bB\varepsilon_{xx}/2BkT << 1$, then the denominator in the definition for the degree of polarization can be approximated by

$$L_{\parallel} + L_{\perp} = L_{\parallel hh} + L_{\parallel lh} + L_{\perp hh} + L_{\perp lh}$$
$$\approx (G_{hh} + G_{lh})\left[\int((1-\cos^2\alpha) + (\tfrac{1}{3} + \cos^2\alpha))d\Omega + \int\tfrac{4}{3}d\Omega\right] \qquad (22)$$
$$= \frac{16\pi}{3}(G_{hh} + G_{lh})$$

As a result of strain along the x axis, the degree of polarization can be expressed as

$$\rho = -\frac{3bB\varepsilon_{xx}}{20DkT} \qquad (23)$$

and, for a strain along the y axis, the degree of polarization is

$$\rho = -\frac{3bB\varepsilon_{yy}}{20DkT} \qquad (24)$$

For the combined strain along x and y, superposition of the above expressions gives

$$\rho = -\frac{3bB}{20DkT}(\varepsilon_{xx} - \varepsilon_{yy})$$
$$= K_{\varepsilon}(\varepsilon_{xx} - \varepsilon_{yy}) \qquad (25)$$

This expression relates degree of polarization to applied strain, assuming that the crystal

is highly isotropic. The strain elements can be replaced by stress parameters. The degree of polarization is then

$$\rho = -\frac{3bB(1+\nu)}{20EDkT}(\sigma_{xx} - \sigma_{yy}) = K_\sigma(\sigma_{xx} - \sigma_{yy}) \tag{26}$$

where ν is Poission's ratio, E is Young's modulus and σ_{xx} and σ_{yy} are the stress components along the x and y axes, respectively. Evidently, DOP can be related to strain or stress. However, stress is more easily determined in experiments. The value for K_σ has been found experimentally to be $-(5.1 \pm 0.3)\times10^{-11}$ cm^2/dyn for GaAs, and $-(9.4 \pm 1.0)\times10^{-11}$ cm^2/dyn for InP [8]. The reader should note that the theory relating strain in semiconductor energy bands to the luminescent properties of a crystal still requires further development. In this work, calculations to convert DOP values into stress values assumed the experimentally determined parameter K_σ for GaAs.

It is important to note that the relationship between degree of polarization and the difference in the stress components has been investigated for stresses up to approximately 2.7×10^9 dyn/cm^2. It is expected that the relationship is non-linear for higher values of stress. However, for the experiments in this work, measurements of σ_{xx}-σ_{yy} were well below the maximum value.

In general, for a semiconductor bonded uniformly in a plane parallel to the xz

plane, the stress created along the x axis would be much greater than the stress along the y axis, i.e., $\sigma_{xx} >> \sigma_{yy}$. The forces involved in the bonding process are created when the laser cools to room temperature from the bonding temperature, and the magnitude of the forces parallel to the plane of bonding is significantly larger than the perpendicular forces. Thus, the mechanical stresses discussed in the experimental results of this thesis can be approximated as σ_{xx}.

Chapter 3 Bonding Analysis

3.1 Introduction

Mechanical stress in diode lasers can generate many outcomes, such as altered optical properties and threshold currents [3]. Stress may also reduce the useful lifetime of devices [4-6]. In this work, the influence of bonding on the lifetime of GaAs-based lasers was studied. GaAs-based laser chips were bonded to oxygen-free high-conductivity (OFHC) copper heat sinks using eutectic PbSn solder or Ablebond silver filled epoxy. Devices were life tested and measurements were taken of the degree of polarization (DOP) of photoluminescence on the output facets to observe stress in the lasers [8]. Lasers were also bonded to OFHC Cu, CuW (Cu-15%,W-85% by nominal weight) [23] or Kovar (Ni-29%, Co-17%, Fe-54%, by nominal weight) [24] heat sinks using PbSn solder or Ablebond epoxy, and DOP measurements were taken at the facets to determine bonding stress in the laser material.

The curing process for many epoxies consists of a temperature-time combination. That is to say, while an epoxy can be cured over a specified time, at a specified

temperature, it can also be considered cured in a shorter time, at a higher temperature. If a laser chip is to be bonded to a heat sink using a conductive epoxy with this characteristic, one must consider the possible results due to the range of temperatures that the laser is exposed to. Effects of three different curing temperatures of 80°C, 125°C and 200°C were also studied on GaAs-based lasers bonded to Kovar heat sinks with ME 8412 conductive epoxy.

This work compared bonding adhesives through visual inspection and DOP measurements. Distribution of the solder and Ablebond epoxy in packaged lasers was observed in scanning electron microscope (SEM) images. DOP measurements were also obtained from the photoluminescence of the active layer to study the corresponding stress variations as a result of adhesive distribution. Voids within the bonding layer of a packaged laser have been observed in SEM images, and resulting stress at the output facet has been studied in DOP mapping.

Analysis of DOP is an effective method for determining patterns of stress in semiconductor materials. Because this technique has been shown to provide information on stresses due to external effects, oxides, bonding, and lattice mismatch [3-14] it is a useful tool for measuring effects caused by die attachment of semiconductor lasers.

3.2 Experimental Details

3.2.1 Life Test

High power GaAs-based diode lasers [25] were processed and life tested at the EG&G Optoelectronics facilities. The lasers were 610 μm long with facet areas of 635 μm × 110 μm, with 300 μm wide active layers and emission wavelengths of 850 nm. Fifty devices were bonded active up to OFHC Cu heat sinks using eutectic PbSn solder at 200°C. Fifty devices were also bonded active up to OFHC Cu heat sinks with Ablebond silver filled conductive epoxy. For the epoxy bonding, an epoxy dot size of approximately 0.010" was placed on the heat sink at room temperature, and a chip was mounted on top. Once the chip was in place, the epoxy was cured at 150°C for 1 hour. All 100 devices were wirebonded, out of stripe, on the p-side and packaged.

In the life test, the devices were driven at 30 A with 150 ns pulses at a 10kHz repetition rate at 25°C for 1000 hours. Output power, forward voltage and wavelength of the devices were measured at 0 hours, 168 hours and 1000 hours. The repetition rate during these measurements was decreased to 1kHz. After 1000 hours of life test a non-parametric statistical test was performed on the change in power and change in forward voltage to estimate the significance of changes in these values for the two groups of lasers.

3.2.2 DOP Measurements and Stress Analysis

Another sample set for this study was prepared by bonding GaAs-based laser chips to different heat sinks with eutectic PbSn solder or Ablebond epoxy. The lasers were 750 μm long, with facet areas of 550 μm × 110 μm, and 230 μm wide active layers with emission wavelengths of 904 nm. The lasers were bonded active up to OFHC Cu, CuW or Kovar heat sinks using either of the bonding adhesives. In this part of the experiment, the lasers were only bonded to the heat sinks, and not wirebonded on top. For the solder, eight chips were bonded to OFHC Cu heat sinks, nine to CuW heat sinks and four to Kovar heat sinks. For Ablebond epoxy, nine chips were studied with the OFHC Cu heat sink, eight with the CuW heat sink, and four with the Kovar heat sink.

To observe the effects of different curing cycles on the bonding process of lasers, laser chips were mounted active up on Kovar heat sinks using a second silver filled conductive epoxy (ME 8412). Three lasers were mounted with the epoxy cured at 80°C for 16 hours, four lasers with the epoxy cured at 125°C for 2 hours, and three lasers with the epoxy cured at 200°C for 10 minutes.

Photoluminescence measurements were obtained using the apparatus illustrated in Figure 3.1. In general, for such measurements, HeNe laser light is mechanically chopped with an optical chopper (Stanford Research Systems Model SR540), and is directed

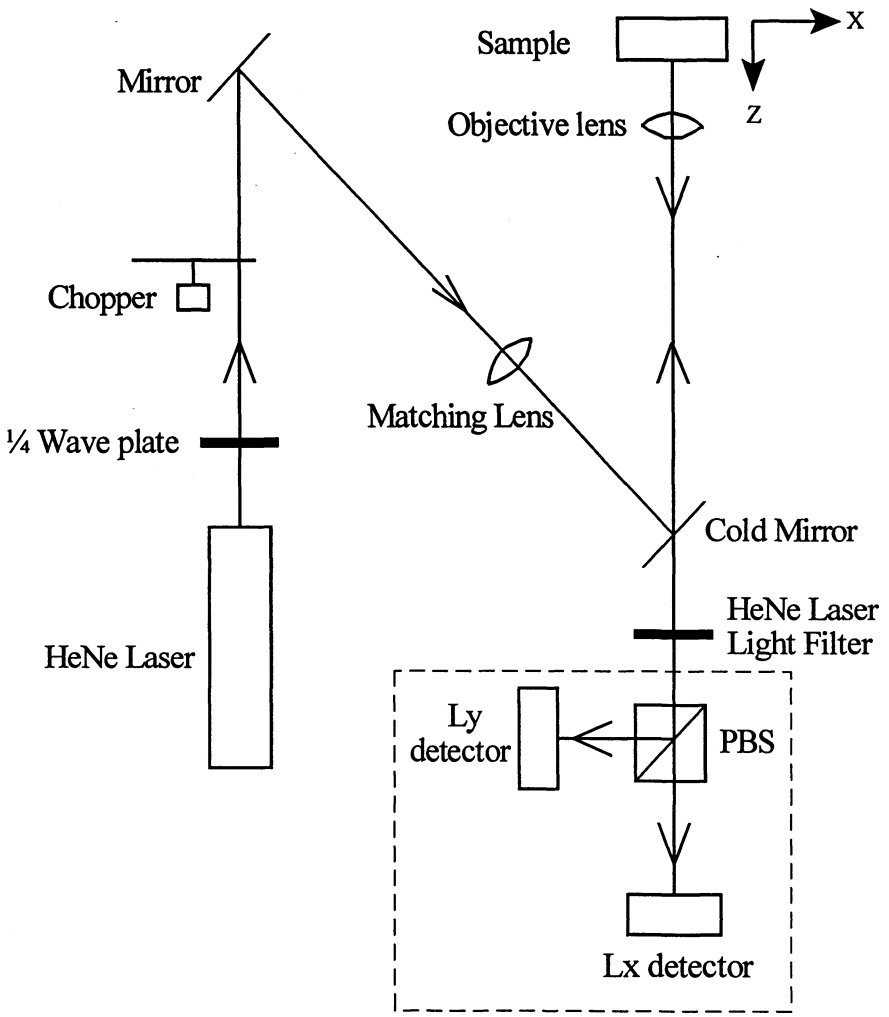

Figure 3.1 Apparatus for degree of polarization measurements.

through a microscope objective lens (Newport M-10X) which focuses the incident HeNe laser light on the semiconductor material being studied. A quarter-wave plate is placed at the HeNe laser to prevent back reflections into the laser tube. To minimize chromatic aberrations caused by the HeNe laser and photoluminescent light, a matching lens is used. The luminescent light and the reflected HeNe light pass through the objective lens. The HeNe light is attenuated by a cold filter (Melles Griot 03 MCS 005) and a HeNe laser light filter (Melles Griot 03 FCG 111), and the remaining photoluminescence passes to a detector module with a polarizing beam splitter (Meadowlark PBS Type III) and two Si p-i-n photodetectors (EG&G C30807E) that measure the irradiances of the resolved polarization components. This technique has been shown to have a spatial resolution of about 1 μm, and a strain resolution of 10^{-5} [12]. The polarizing beam splitter cube possessed wavelength dependence. In other words, the cube transmitted L_x polarization to the L_x detector, but some fraction of the L_x polarization would also be reflected to the L_y detector. This fraction was wavelength dependent. Thus, a calibration technique established by Jian Yang was implemented to accommodate the wavelength dependence [26].

Experiments have shown a relationship between the DOP measured from photoluminescence of a III-V semiconductor and the mechanical stresses σ_{xx}-σ_{yy} in the semiconductor as

$$DOP = K_{\sigma}(\sigma_{xx} - \sigma_{yy}) \quad (1)$$

where the terms in parentheses describe the local stress in the region emitting the photoluminescence and K_σ is a constant which depends on material properties. The constants have been reported to be $-(5.1\pm0.3)\times10^{-11}$cm^2/dyn for GaAs, and $-(9.4\pm1.0)\times10^{-11}$cm^2/dyn for InP [8]. For a device bonded uniformly to a plane, we expect $\sigma_{xx} >> \sigma_{yy}$. Thus, in the case of GaAs, a measured DOP of 1% would correspond to a stress of $(2.0 \pm 0.1) \times10^8$ dyn/cm^2.

Data was obtained by mapping photoluminescence of a sample. The sample was placed on a stage with XYZ motion that was controlled by motors (Oriel Motor Mike) which were driven by computer-based software. For each XY position for the sample, irradiances of the resolved polarizations was measured from the Si detectors and stored in the computer which then calculated the DOP.

For bonding measurements, DOP mapping was obtained over a width of 40μm to 50μm and a height of approximately 110μm, which was the thickness of the laser chips. The area scanned was approximately the centre of the output facet of the laser. For each scan, the steps between measurements were usually 2 μm. Bonding stress was compared by calculating the mean DOP value over an area 40μm-50μm × 14μm near the bonded region.

Two lasers were prepared for DOP mapping of a plane parallel to the active layer. Both lasers had been bonded to OFHC Cu heat sinks; one was soldered and the other was bonded with Ablebond epoxy. The lasers had not been wirebonded. Both lasers were soaked in an $HF:H_2O$ (1:5) solution for 2 hours to remove the Au/Pt/Ti top metal layers and dielectric. They were then etched in $H_2SO4:H_2O_2:H_2O$ (1:12:150) for 2.5 minutes to remove approximately 5 μm of GaAs. After this process, the plane of the active layer of both lasers was accessible for DOP measurements. For each scan, the steps between measurements were usually 5 μm. The areas scanned were 550 μm × 750 μm.

3.3 Results and Discussion

3.3.1 Life Test Results

During the course of the life testing, it was found that the median decrease in power for the fifty soldered devices was 15 W, and the median decrease in power for the fifty epoxied devices was 25 W. Thirty-six of the lasers mounted with Ablebond epoxy and twenty of the soldered devices produced minimal levels of power after operating for 1000 hours. There was no statistically significant difference in change in the forward voltage in the life test, indicating that the operating conditions for the laser were not altered significantly during the life tests. From these results the non-parametric statistical test [27] shows that, with 90% confidence, the mean lifetime of the devices mounted with Ablebond epoxy is less than the mean lifetime of the devices that have been solder-

bonded.

3.3.2 DOP Measurements and Stress Analysis

From DOP measurements, stress has been observed to depend on the bonding adhesive. For twelve of the life tested GaAs-based lasers, mean DOP values of 1.6 ± 0.4% and 4.6 ± 1.0 % were found for solder-bonded devices and Ablebond epoxy-bonded devices, respectively, where the uncertainty is one standard deviation of the mean. The data indicate that Ablebond epoxy-bonded devices experienced on average higher levels and more variation of stress than the solder-bonded devices.

The stress patterns between the two types of packaged lasers are shown in Figure 3.2 and Figure 3.3. The side bonded to the heat sink is on the bottom of each image. In the maps, regions under compression with respect to the horizontal axis are blue, while the regions in tension are red, assuming $\sigma_{yy} << \sigma_{xx}$. Low strained, or unstrained regions are green. Figure 3.2 (a) is a facet map of a soldered laser which exhibited good power after 1000 hours of life testing. The image showed low strain overall, with little compression near the bonded region. In Figure 3.2 (b), a soldered laser which failed had slightly more compression near the heat sink. As a comparison, Figure 3.3 (a)-(b) showed the higher stress resulting from lasers that had been bonded with epoxy. The stress patterns observed using degree of polarization resembled the stress patterns seen

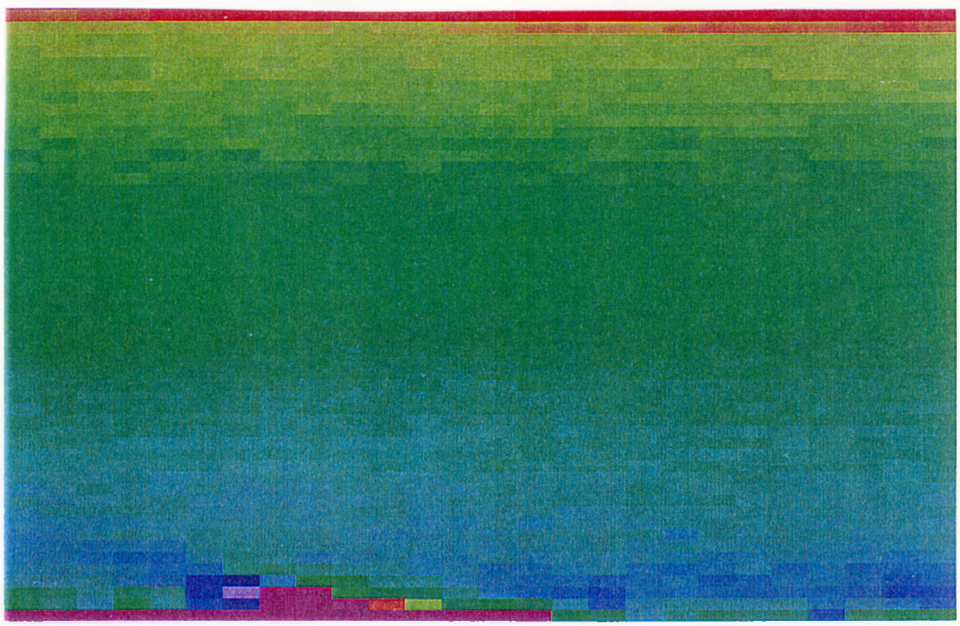

(a)

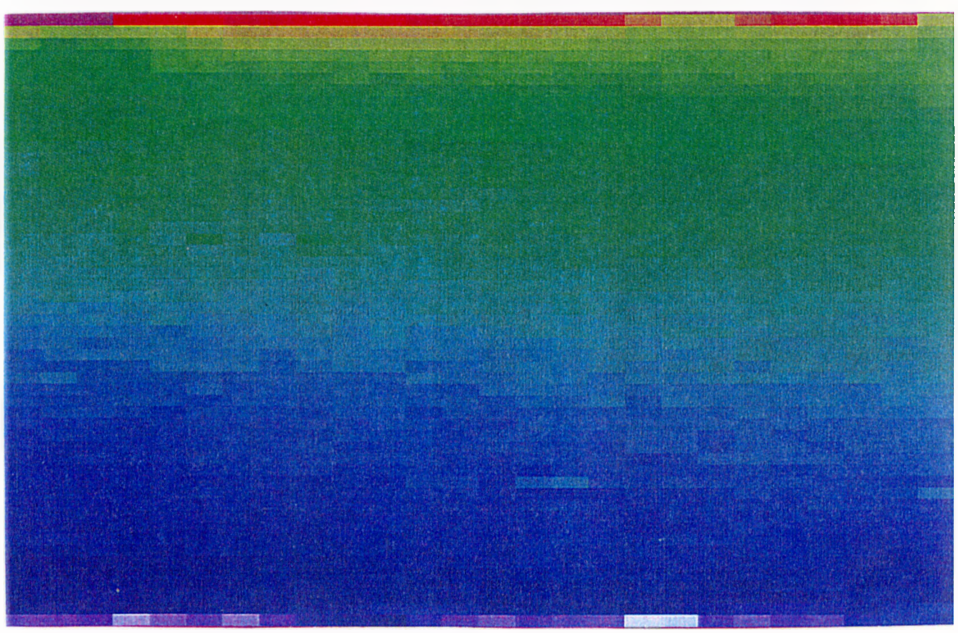

(b)

Figure 3.2 DOP facet images of lasers from life test. The images correspond to a soldered laser which passed (a) and one that failed (b).

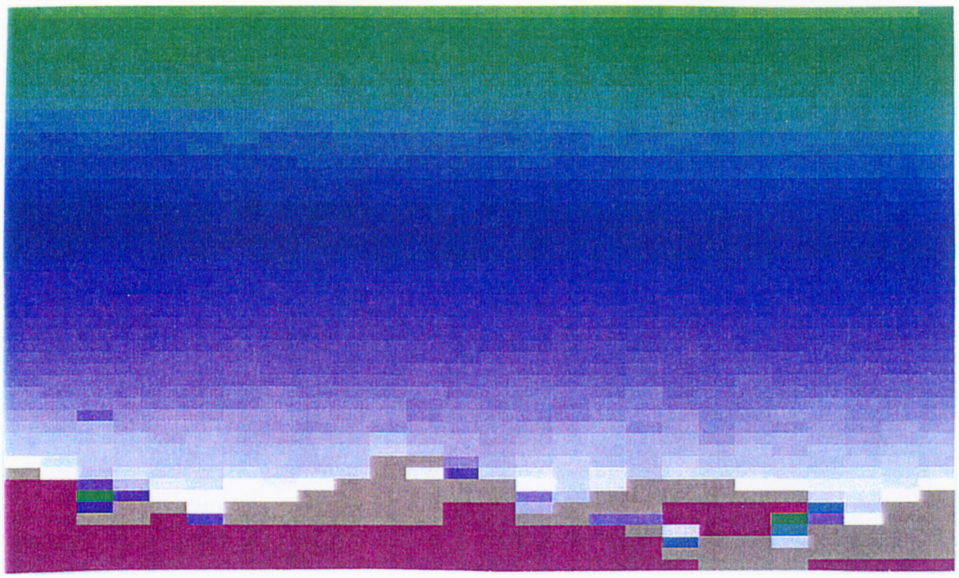

(a)

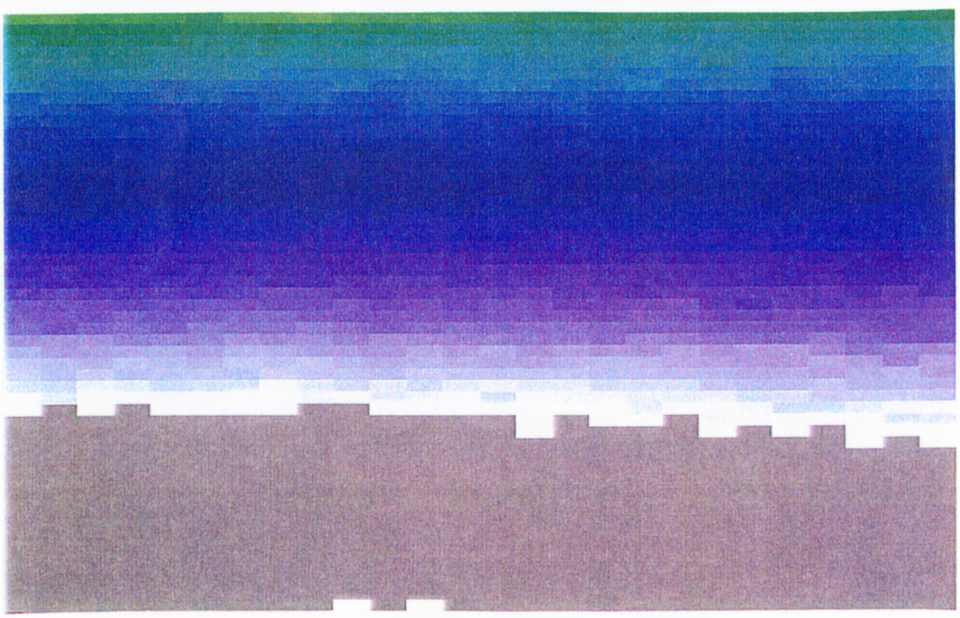

(b)

Figure 3.3 DOP facet images of lasers from life test. The images correspond to a laser bonded with Ablebond epoxy which passed (a) and one that failed (b).

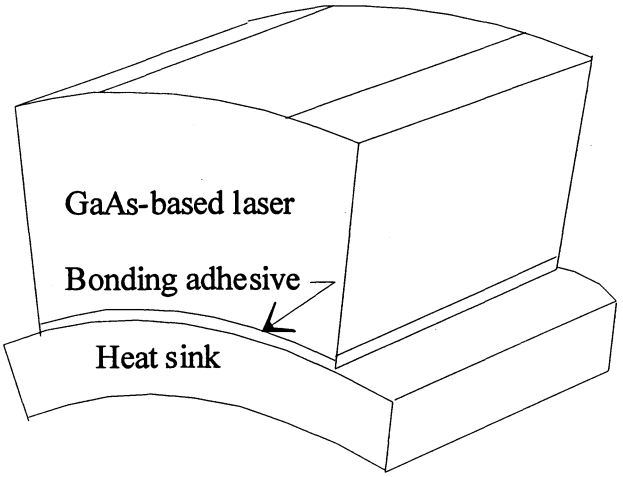

Figure 3.4 Sketch illustrating the 'bending' of the laser as a result of bonding to the heat sink.

for a uniform beam bending, as illustrated in Figure 3.4. This simplification has been shown to be useful by approximating the stress in the bending of a uniform beam.

DOP mapping has also shown that stress depends on the combination of materials used in the bonding process. The parameter by which the effects of stress were compared was the coefficient of thermal expansion (CTE). Table 3.1 outlines the reported values of CTE for the materials used in this study. Bonding stress was decreased in cases where the heat sinks had coefficients of thermal expansion (Figure 3.5) closer to that of the laser material. Higher levels and more variation of stress were induced by Ablebond epoxy. Although Kovar is reported to have a CTE less than that of GaAs, the compressive stress

shown in Figure 3.5 may be caused by the combination of metalization and adhesion

Material	CTE (ppm/°C)
GaAs[28]	6.4
OFHC Copper[29]	16.6
CuW[23]	7.0
Kovar[23]	5.9
Eutectic PbSn Solder[30]	25
Ablebond Epoxy[31]	130
ME 8412 Epoxy[32]	45

Table 3.1 CTE values for the various materials used in this study.

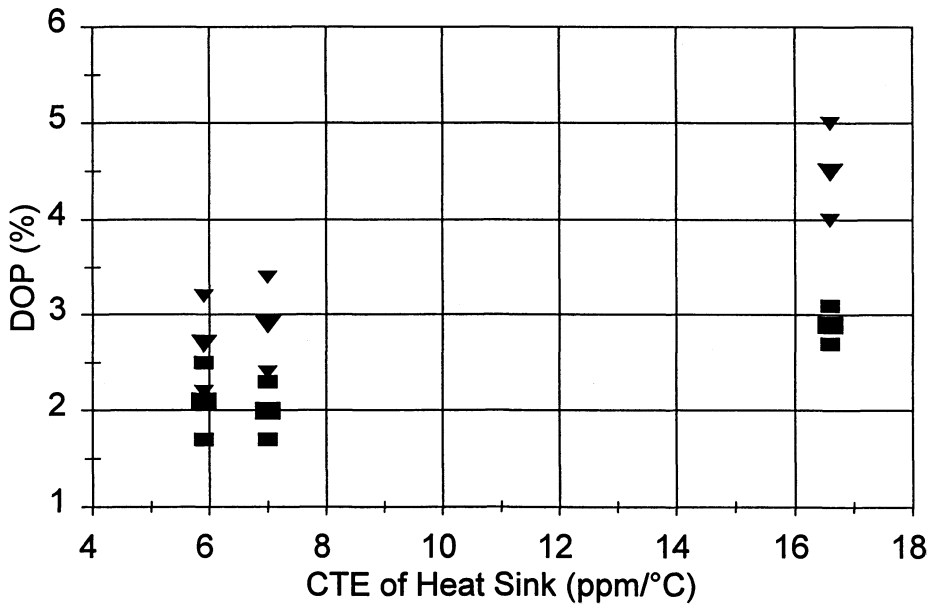

Figure 3.5 Mean DOP values calculated in n-region of lasers bonded to heat sinks with eutectic PbSn solder ▬ and Ablebond epoxy ▼.

stress. Because the CTE of this epoxy at the curing temperature was much higher than that of the laser material and the heat sinks, the bonding stress may have been high enough to degrade the reliability of the laser. For many epoxies, curing can occur above the glass transition temperature, at which point the properties of the epoxy change such that the epoxy becomes a much more hardened substance. As the reported glass transition temperature of Ablebond epoxy is 90°C, and the curing temperature used in this case was 150°C, the curing probably produced a strong and rigid adhesive that strained the laser material significantly. The above results suggest that the bonding adhesive, as well as the heat sink, may affect the overall performance of the laser.

Experimental observations of ME 8412 epoxy have shown that curing temperatures may affect the bonding of the lasers. For the curing temperatures of 80°C, 125°C and 200°C, the average DOP values near the region of bonding was 0.3 ± 0.1%, 1.2 ± 0.3%, and 0.7 ± 0.2%, respectively, where the uncertainty is one standard deviation of the mean. The data show that the lower curing temperature results in lower stress near the bonding region. For the samples that were mounted with the epoxy cured at 200°C for 10 minutes, the average DOP values near the bonding region were slightly lower than those bonded at 125°C. Assuming that the parent distribution describing these measurements is normal, a 1-tailed t-test on the measurements at 125°C and 200°C

reveals that the probability of the 200°C cure producing the same DOP values as the 125°C cure is 0.07, suggesting that the results are not likely the same. For the 10 minute curing time, it is difficult to determine if the epoxy maintained a temperature of 200°C. Despite the difference between the effects of the higher curing temperatures, the results indicate that curing conditions can contribute to the overall bonding stress in the laser.

The DOP images in this experiment resembled the stresses caused by the bending of a uniform bar where the surface bonded to the heat sink was under compression and the top of the chip experienced compression. Although the devices have been assembled with the active region up, the bonding stress caused at the interface of the n-side and the heat sink had an effect on the stress in the active region. Figure 3.6 illustrates the range of DOP values that have been measured along the front facet of lasers studied in these experiments. The top of the chip corresponds to 0μm and the bottom of the chip corresponds to 110μm. For the chip bonded at 80°C, both compressive and tensile stresses along the laser facet are low, and the range of DOP values along that sample is approximately 0.5%. For the chip bonded at 125°C, the range of stress values along the output facet is larger, with the range in DOP being approximately 1.9%. Figure 3.6 also shows a comparison of the effects caused by the two epoxies. While the range of DOP values for the chips bonded with ME 8412 were 0.5% and 1.9%, an Ablebond epoxied laser that failed in the life test shows a range of approximately 3.4%. Thus, the bonding

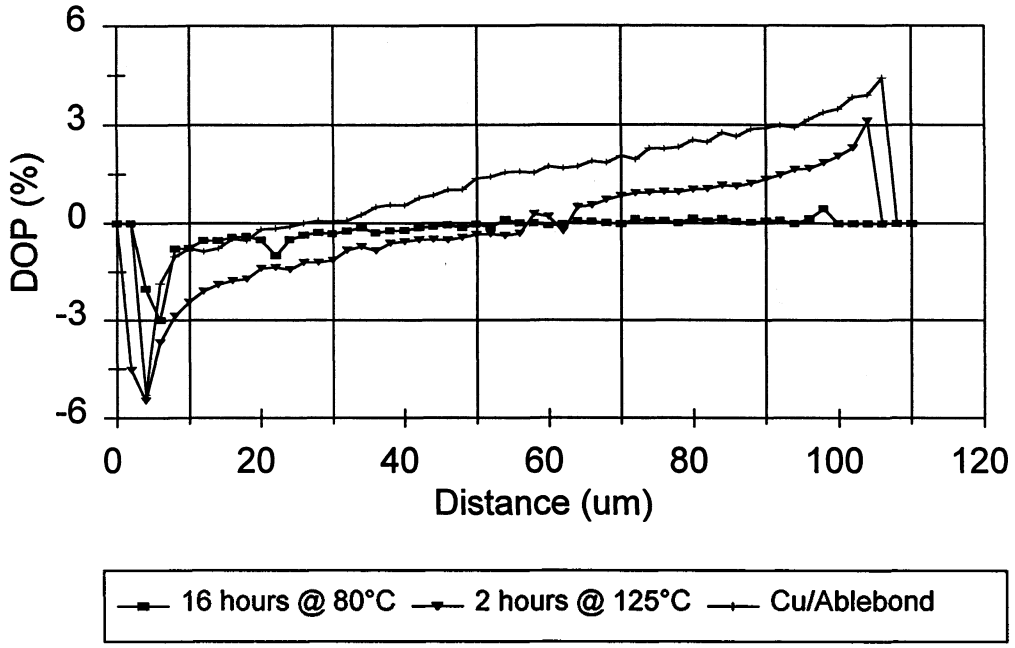

Figure 3.6 DOP ranges along the front facet of lasers bonded with Ablebond or ME 8412 epoxies.

process originating in a region on the n-side of the laser also affected the active layer.

It should be noted that the overall stress along the bonded region of lasers bonded with ME 8412 epoxy was less than the stress caused by the Ablebond epoxy or the eutectic PbSn solder. Life testing on lasers bonded to Kovar heat sinks with ME 8412 epoxy resulted in fewer failures than lasers bonded to Kovar heat sinks with eutectic PbSn solder. Although the coefficient of thermal expansion for the ME 8412 epoxy was slightly larger than the eutectic PbSn solder, the bonding processes were still different. Soldering took place over a few minutes, while curing of ME 8412 took place over 16

hours, allowing for relaxation of the materials during bonding.

The difference in the distribution of the bonding adhesives was investigated. One soldered chip (Figure 3.7 (a)) and one chip bonded with Ablebond epoxy (Figure 3.7 (b)) were examined under a scanning electron microscope. The solder appeared to distribute itself uniformly between the heat sink and laser material. This is the result of the characteristic wetting of solder. However, the Ablebond epoxy tended to accumulate around the edges of the chip. There was no precise control of the dispensed epoxy dot size, or of the pressure applied to the chip when bonding. Therefore, the accumulation below and around the chip varied, resulting in uneven bonding.

The penetration depth of DOP measurements is approximately 100 nm. Thus DOP images of the front facet of lasers provided only some information about the bonding stress. Measurements of DOP were obtained in the plane of the active layer for two lasers, and the results are shown in Figure 3.8. Distribution of the stress caused by the bonding adhesive was observed along the entire length of the laser for a soldered sample (Figure 3.8 (a)) and an Ablebond epoxied laser (Figure 3.8 (b)). The top of each image corresponds to the front facet. For the lasers that were etched to the active layer, the soldered laser exhibited low values of DOP. However, the laser that had been bonded with epoxy had uneven distribution of stress, with low DOP near the front and back

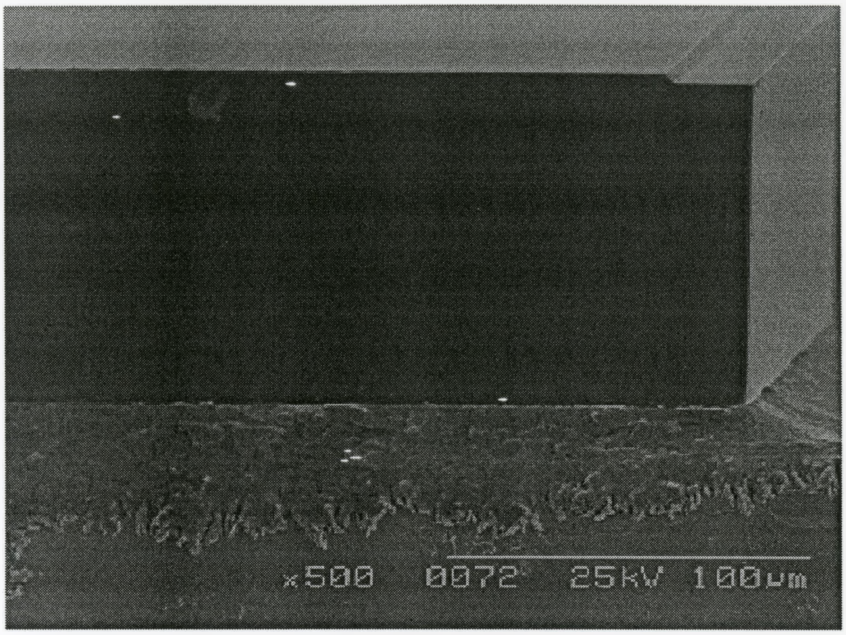

(a)

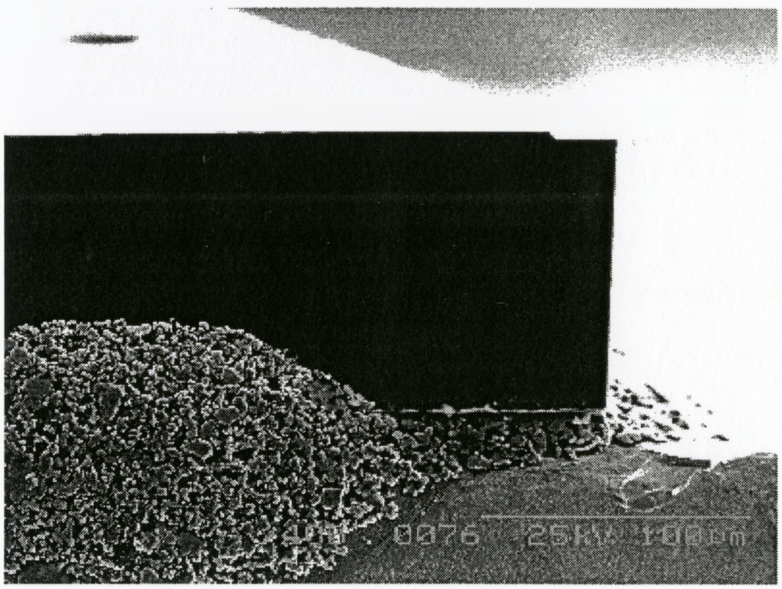

(b)

Figure 3.7 Scanning Electron Microscope images showing distribution of a eutectic PbSn solder (a) and Ablebond epoxy (b). The solder is distributed uniformly in the bonding layer while the epoxy accumulated in some regions.

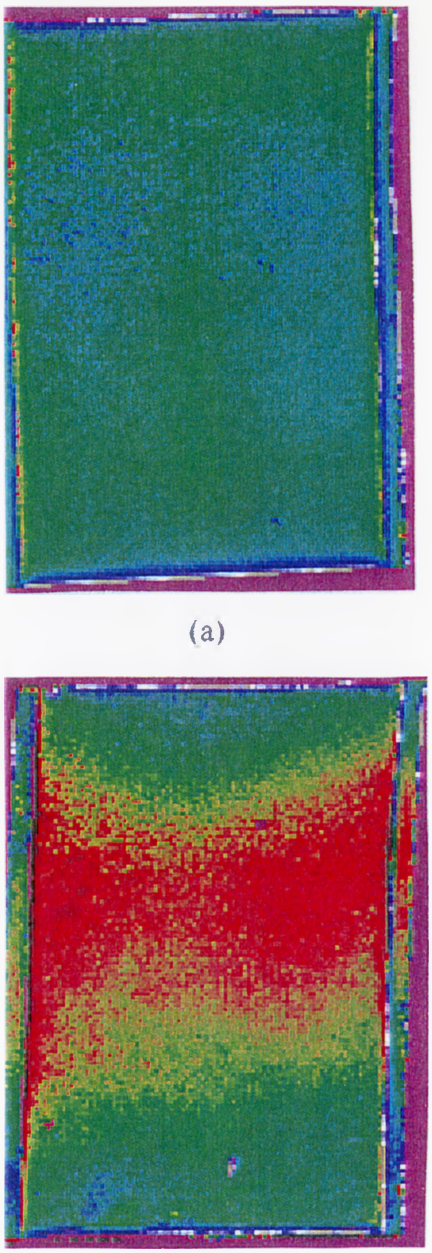

(a)

(b)

Figure 3.8 DOP images of the top view of GaAs-based lasers etched to the active layer, comparing a laser bonded with (a) eutectic PbSn solder and a laser bonded with Ablebond epoxy (b).

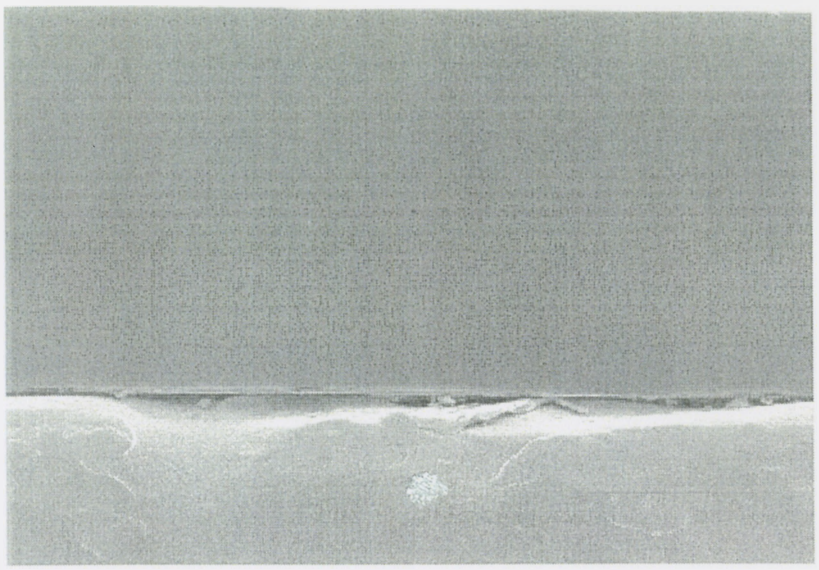

(a)

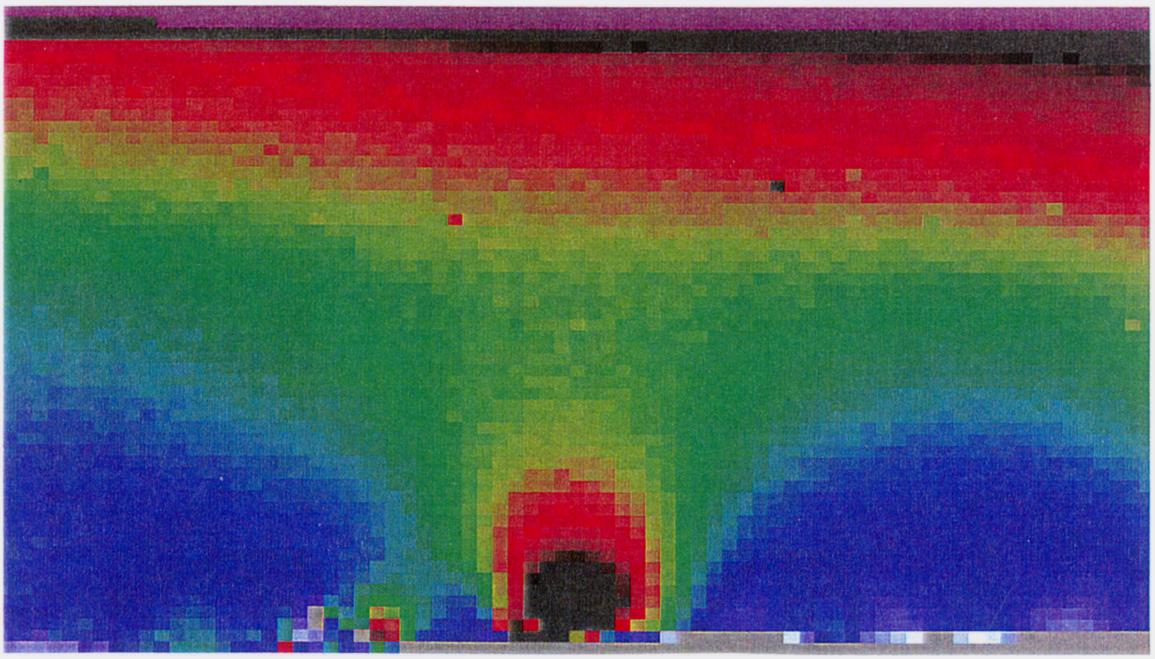

(b)

Figure 3.9 Scanning electron microscope image of voids in the Ablebond epoxy layer (a) and the resulting DOP image of the front facet (b).

facets, but high tensile stress through the centre of the chip. The lasers had not been wirebonded, nor had they been operated, which minimized possible sources of stress in the semiconductor. The maps suggest that the uneven distribution of epoxy around the chip led to variations in the stress within the chip.

The effect of voids in the bonding layer was investigated on a laser bonded to an OFHC Cu heat sink using Ablebond epoxy. Voids can be described as a reduction in thermal conductivity within the bonding layer. This would normally be the result of an air pocket present in the adhesive. An SEM photo of the bonded laser chip shows voids in the bonding layer near the output facet (Figure 3.9 (a)). The stress patterns arising from the voids on this device can be seen in Figure 3.9 (b). The image displays a DOP image with an offset of about 3% simply to show the variation in the measurements. Although the void was small in the bonding layer, the resulting stress was not uniform and covered a large region on the facet of the laser.

3.4 Summary

This work has studied aspects of GaAs-based diode lasers with different bonding processes. Initial life test results have shown a low life expectancy for the lasers bonded to OFHC Cu heat sinks using Ablebond conductive epoxy. The degree of polarization measurements indicated that the type of heat sink and bonding adhesive affected the

stress in the laser material. It was observed that a larger mismatch of CTE of the materials used induced higher levels of stress. Lasers bonded to Kovar heat sinks with ME 8412 epoxy exhibited better performance than the lasers bonded to Kovar with eutectic PbSn solder. In addition, physical aspects, such as adhesive distribution and voids, of the bonding adhesives were studied to obtain further insight into their effects on bonding stress. Results suggest that the effects of the bonding adhesive on reliability should be considered in the design of chip packaging.

Chapter 4 Applied Force Measurements

4.1 Introduction

Experiments have shown that mechanical stress in diode lasers can affect laser performance. However, little is known about the direct relationship between the amount of stress in a laser diode and the resulting performance and reliability of the device, and more importantly, the maximum amount of stress that a laser can tolerate without exhibiting significant degradation. In this experiment, the effect of stress on the rate of degradation of lasers was studied. This was achieved by mounting a bare GaAs-based diode laser chip centred on a groove in a copper plate, and applying various forces to the chip. Output power was measured as a function of time to observe rates of degradation at the different applied forces. To relate the rate of degradation in a laser to the stress within the laser, DOP was measured from the photoluminescence of the front facet of the lasers, with various applied forces. Measurements obtained in this experiment provided insight into stress tolerance to help the design and to understand reliability of the lasers.

4.2 Experimental Details

4.2.1 Degradation Measurements

The experimental setup consisted of two major components which were the adjustable probe connected to a laser driver, and a copper plate and thermo-electric cooler combination. A groove was prepared on a copper plate (Figure 4.1) which was mounted on a thermo-electric cooler. The copper was approximately 2 mm thick, and was cut to a 10 mm × 10 mm plate which was polished with 4000 grit SiC paper. A diamond saw

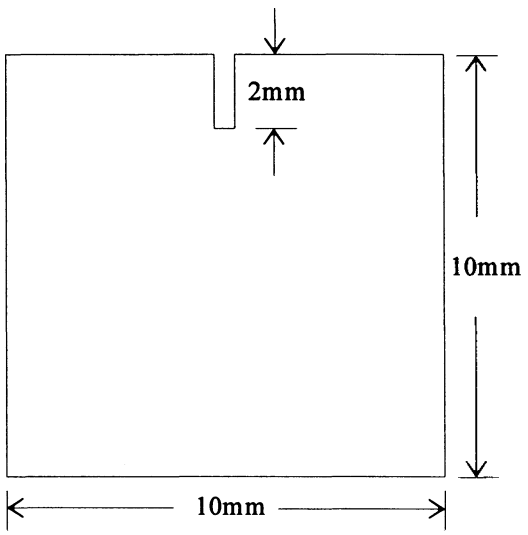

Figure 4.1 Copper plate with groove used for applied force measurements.

blade of 0.015" diameter was used to make the groove 2 mm into one side of the copper plate. The plate and groove were smoothed with sand paper, then polished further with SiC paper. The copper plate was affixed to the thermo-electric cooler using a thermally conductive epoxy (Wakefield Delta Bond 155), which was cured for 24 hours at room

temperature. The thermo-electric cooler was mounted on an aluminum base which was secured to an XYZ translation stage (Newport 460 XYZ Series) for alignment, and was kept stationary for measurements.

The probe had been sanded to a point of about 50 μm radius of curvature using SiC paper [20]. It was suspended firmly on a plexiglass mount which was attached to a bar of aluminum (Figure 4.2). A strain gauge was secured to the aluminum bar such that a force applied to the probe would cause the aluminum bar, and hence the strain gauge, to

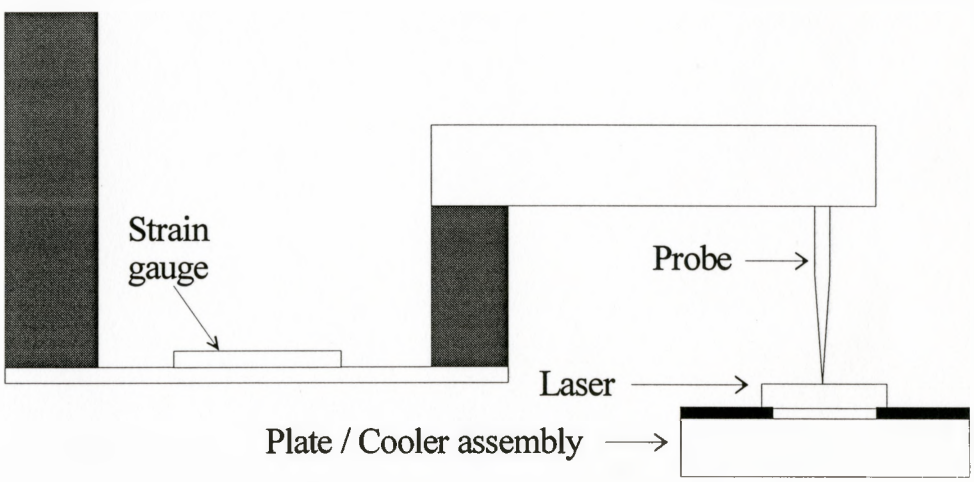

Figure 4.2 Probe assembly used for applied force measurements.

bend. The assembly was secured on an XYZ translation stage which was kept stationary during measurements.

Contacts were located at the copper plate, and at the probe which applied various forces to the chip. These contacts were connected to a laser driver (DEI LDX-P-100A) that included a current monitor circuit. Current supplied to the chip was monitored from the circuit by means of an SMB connection to an oscilloscope (Hewlett Packard 54600 A). A reference signal from the laser driver was also directed to a standard phase locked

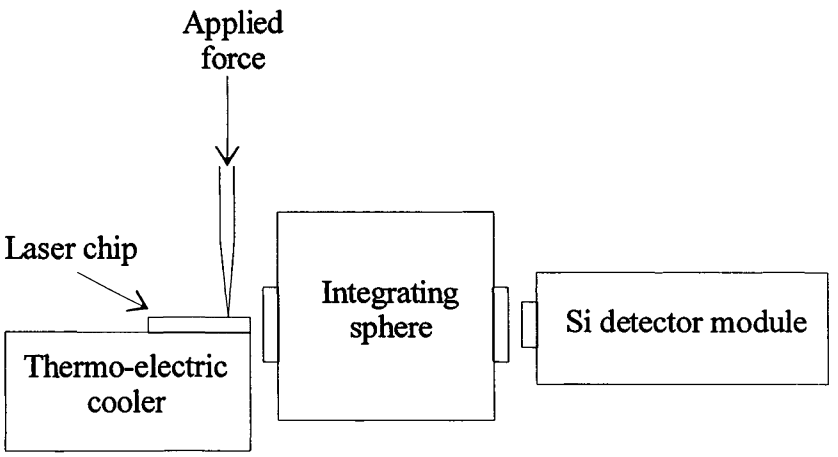

Figure 4.3 Alignment of laser to detector module using an integrating sphere.

loop circuit, which provided a phase reference for the PC-mounted phase sensitive detector (PC-PSD). The input to the PC-PSD was connected to a Si p-i-n photodetector

(RCA 30670 E) with a pre-amplifier. To prevent overloading on the photodetector from the high power output of the laser, an integrating sphere (Labsphere) was aligned between the output facet of the chip and the detector, as shown in Figure 4.3.

Before a chip was mounted to the apparatus, thin gold foil was placed on the copper plate and over the groove to provide good contact between the plate and the chip. The gold foil was approximately 10 mm × 2 mm and 1500 Å thick, and was held in place on the plate by the clamp which served as one of the contacts. The gold foil was held in place approximately 0.5 mm from the grooved edge of the copper plate so that the groove was still visible when mounting a laser. A eutectic PbSn solder preform was also placed at the tip of the probe as another means of improving contact to the chip. A laser chip was mounted, p-side down, over the gold foil so that the chip was centred over the groove, and the output facet of the laser was pointing towards the entrance of the integrating sphere.

All laser chips in this experiment were fabricated and processed at the EG&G facilities and fell under two categories, which were standard lasers taken from batch D462502 and lasers taken from batches QX173B and QX171A, which produced lasers with poor reliability, on average. Laser chips from batch D462502 were 610 μm long with facet areas 635 μm × 110 μm, and active regions 300 μm wide. Chips from batches

QX173B and QX171A were 750 μm long with facet areas 610 μm × 110 μm, and an active layer 230 μm wide. The performance of the lasers was determined from the operation of chips taken from the same batch. Lasers with poor reliability were those that showed a reduction of 25% in power during life testing.

The standard operating conditions for the lasers from batch D462502 were 30A, 150ns current pulses at a repetition rate of 10 kHz at room temperature, and the standard operating conditions for the lasers from batches QX173B and QX171A were 22A, 150ns current pulses at a repetition rate of 10 kHz at room temperature. To avoid severe degradation from heating, the driving current and repetition rate in this experiment were maintained at levels lower than standard operating conditions. As well, the ageing of the lasers in this experiment did not exceed 100 hours. Thus, the results stated in this work can only be quoted for this duration, but the trends can be referred to as approximate guidelines for ageing of lasers over longer periods of time.

4.2.2 DOP Measurements for Applied Forces

To observe the changes in stress that arose from the forces exerted by the probe, DOP was mapped on the output facet of the chips. The copper plate and thermo-electric cooler assembly described for this experiment was placed in the DOP apparatus described in Chapter 2. The probe was also placed in the apparatus such that it maintained a

constant force on the chip during measurements. The mount holding the groove and the probe assembly were secured on a motorized XY translation stage (Melles Griot Nanomotion II). During the DOP mapping, the chip was mounted p-side down on the groove as it had been in the degradation measurements. For each scan, steps between measurements were usually 5 μm horizontally and 2 μm vertically. It is assumed that the stresses induced in the laser chip were such that $\sigma_{xx} >> \sigma_{yy}$.

4.3 Results and Discussion

4.3.1 Degradation Measurements

The first chips studied were from batch D462502. One laser was driven at 21 A and 200 ns pulse widths, with a repetition rate of 1 kHz at approximately 22.5°C and output power was measured as a function of time for different applied forces. All measurements in the experiment were taken at the same temperature. The results are plotted in Figure 4.4. The plot shows that, for increased applied forces, the output power was reduced, and the rate of degradation increased. When the force was removed, the original degradation rate was restored. Results were obtained with a similar chip under the same conditions, but with the repetition rate at 5 kHz (Figure 4.5). Again, with increased applied force, the output power decreased, and the rate of degradation increased, and the degradation rate was restored when the applied force was lowered. Thus, force applied to a laser chip affected the output performance of the laser.

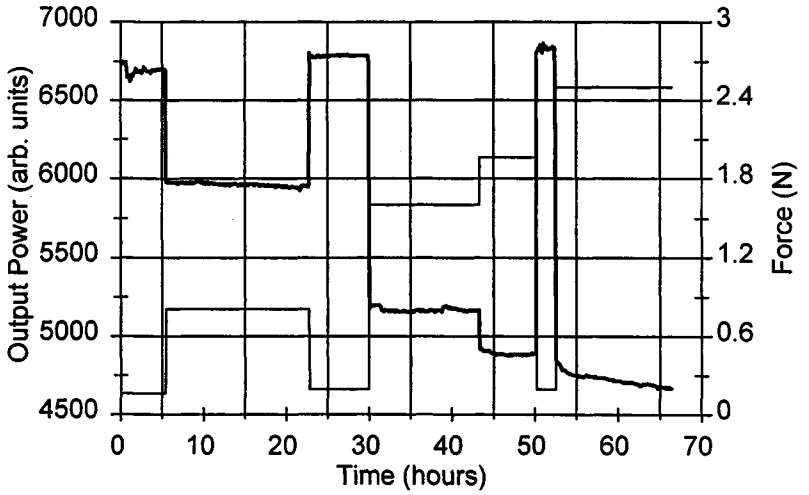

Figure 4.4 Output of a chip from batch D462502 for 1 kHz repetition rate (shown by dark line). The thin line represents the force applied during the experiment.

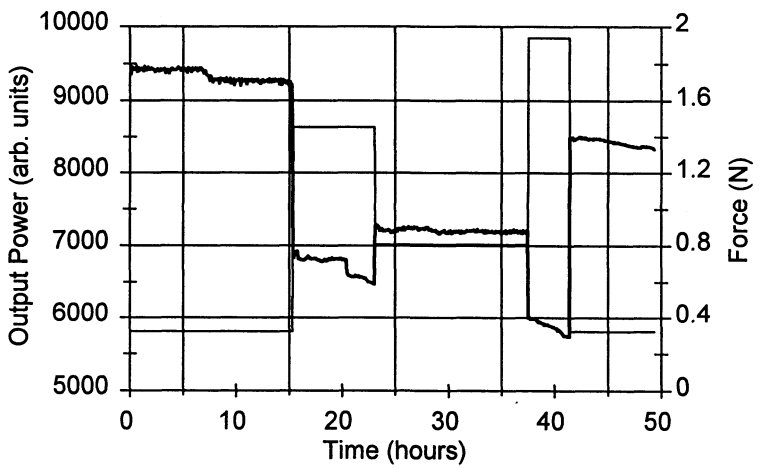

Figure 4.5 Output of a chip from batch D462502 for 5 kHz repetition rate (shown by dark line). The thin line represents the force applied during the experiment.

Chips from the batch that showed poor life were also affected by applied force. For a laser from batch QX173B, the original degradation rate was not restored when the force was reduced. Measurements showed no noticeable correlation between the applied force and the rate of degradation during the first 30 hours of operation for the laser (Figure 4.6). After this point, the degradation rate was found to be 0.97 ± 0.01 %/hour with an applied force of 0.4 N. When the force was increased to 1.4 N, the rate of

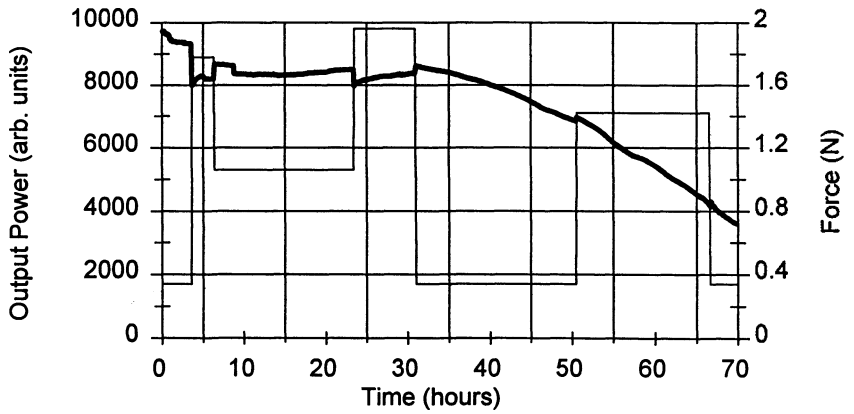

Figure 4.6 Output of a chip from batch QX173B (shown by dark line). The thin line represents the force applied during the experiment.

degradation rose to 1.7 ± 0.1 %/hour. When the force was reduced to 0.4 N again, the original rate of degradation was not restored, but rose to 2.1 ± 0.5 %/hour. To investigate this further, one chip of this type was driven for 68 hours with an applied force of 0.4 N, and another chip was driven under the same conditions, but with the applied force of 2.5 N. Normalized power plotted in Figure 4.7 showed that both chips

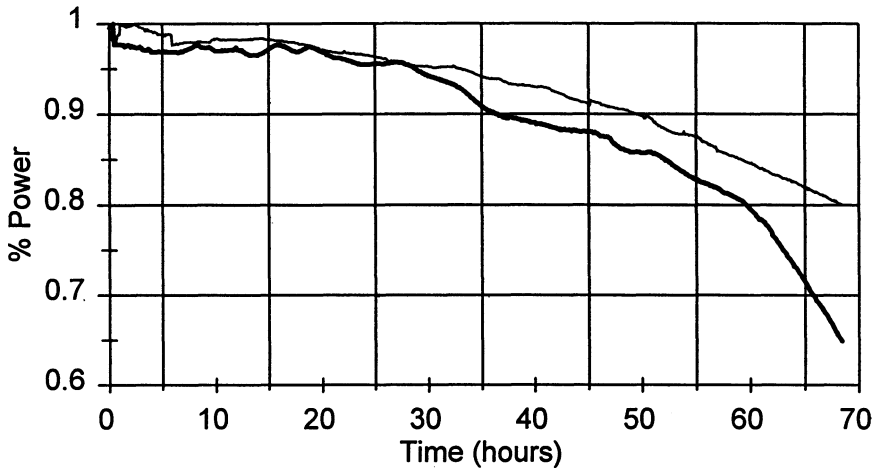

Figure 4.7 Normalized power for lasers from batch QX173B with applied forces of 0.4 N (thin line) and 2.5 N (dark line).

experienced the same rate of degradation for the first 30 hours, but the larger applied force eventually led to a higher rate of degradation after this point, with the power dropping to approximately 65% of its original value. For the lasers from batch QX173B, the degradation accelerated more quickly with a larger applied force, but the degradation was not evident until several hours of operation.

Lasers from batch QX173B were studied with different driving currents. Chips were driven at 14 A, 18 A, or 22 A with 5 kHz repetition rate and 200 ns pulse widths with an applied force of 2.5 N. The degradation rates accelerated after some time of operation, as shown in Figure 4.8. The laser driven at 22 A showed higher

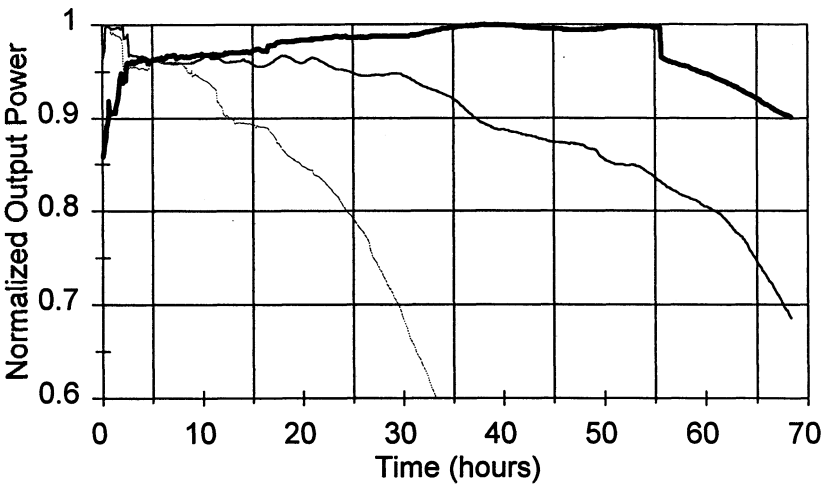

Figure 4.8 Normalized power for lasers from batch QX173B driven at 14 A (dark line), 18 A (thin line) and 22 A (broken line).

degradation than the lasers driven at 18 A or 14 A. Lasers from the poor batch QX171A were also seen to degrade more quickly when driven at higher current pulses with a constant applied force of 2.5 N. The observations were consistent with the expected increase in degradation with exposure to higher current.

The results in this work are reported for lasers that have been mounted active-side down on the groove. However, measurements with these chips have also shown that higher applied forces for chips mounted active-side up on the groove resulted in higher degradation rates. Thus, results suggest that compressive or tensile strains in the active

layer can affect the lifetime of the lasers.

4.3.2 Degree of Polarization Measurements for Applied Forces

Full facet DOP scans were obtained on a chip taken from batch D462502, with various forces applied to the chip. Figure 4.9 illustrates the changes that occur in the output facet with applied probe forces ranging from 0 N to 1.6 N. Compressive stress with respect to the horizontal axis is indicated by blue colours, while tensile stress is shown with red. Low values of DOP are shown by green. As the probe force was increased, the tensile and compressive stresses became more pronounced through the facet. When no force was applied to the chip, the photoluminescence of the front facet showed some tensile strain in the active region had already been introduced, and some compressive strain was introduced in the n-doped side. These strains may have been a result of the metalization of the laser.

A summary of DOP measurements for the laser from batch D462502 can be found in Table 4.1. The DOP values that were calculated in the active region were averaged over an area 60 μm wide and 14 μm high, approximately 4μm from the edge. The DOP values that were calculated in the n-side of the facet were averaged over an area 60 μm wide and 14 μm high, approximately 8 μm from the edge. The areas averaged were approximately in the centre of the output facet as shown in Figure 4.10. For the forces

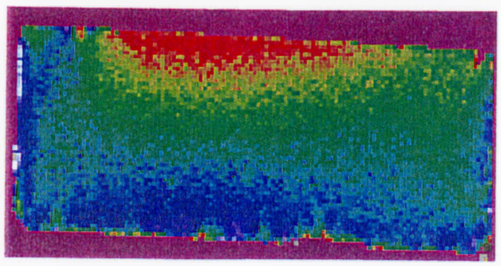

(a)

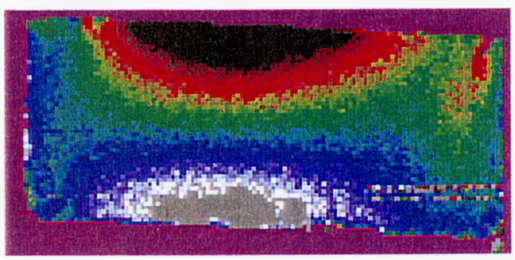

(b)

(c)

Figure 4.9 DOP images of unbonded GaAs-based lasers from batch D462502 with (a) 0 N, (b) 0.9 N and (c) 1.6 N applied forces.

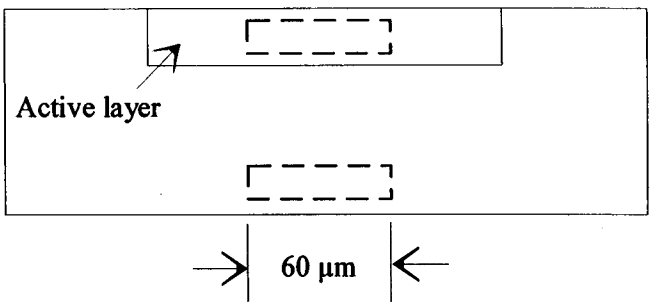

Figure 4.10 Schematic of a DOP scan, locating areas for DOP measurements (denoted by broken lines).

listed, corresponding stress values, σ_{xx}, are included, which were calculated using the constant K_σ (-(5.1 ± 0.3) × 10^{-11} cm^2/dyn) for GaAs. As mentioned earlier, it is assumed that $\sigma_{xx} >> \sigma_{yy}$. The stresses in the active layer were also approximated using the formula for a simply-supported rectangular beam [33]

$$\sigma_{xx} = \frac{6Fw_1w_2}{lh^2(w_1 + w_2)} \qquad (1)$$

where F is the applied force, w1 and w2 are the horizontal distances from the probe to the supports, *l* is the length of the laser, and h is the thickness of the laser. These calculated values are also included in Table 4.1.

Force (N)	Calculated σ_{xx} ($\times 10^8$ dyn/cm^2)	Active layer		n-side	
		DOP (%)	σ_{xx} ($\times 10^8$ dyn/cm^2)	DOP (%)	σ_{xx} ($\times 10^8$ dyn/cm^2)
0	0	-1.4 ± 0.4	2.7 ± 0.8	1.1 ± 0.5	-2 ± 1
0.4	3.3	-4.0 ± 0.7	8 ± 1	3.3 ± 0.6	-6 ± 1
0.9	7.4	-8 ± 1	16 ± 2	7 ± 1	-14 ± 2
1.6	17	-11 ± 2	22 ± 4	10 ± 1	-20 ± 2
2.1	21	-14 ± 2	27 ± 4	13 ± 2	-25 ± 4

Table 4.1 Stress measurements for D462502 laser chip under various forces.

The trends in Table 4.1 show that increased applied force led to an increase in the stress in the laser. All measurements showed that DOP was proportional to the applied force. Thus, compressive stresses up to at least about -(25 ± 4) $\times 10^8$ dyn/cm^2 and tensile stresses up to (27 ± 4) $\times 10^8$ dyn/cm^2 can be measured using this technique. Calculations of stress in the active layer were similar to the approximate stresses obtained for a simply-supported rectangular beam. The results in Table 4.1 also reflect the symmetry in the stress because tensile and compressive stresses were approximately equal in magnitude in the p- and n-regions, respectively.

For the lasers from batch D462502, the applied force recorded during degradation measurements was converted into DOP values in the n-region. The relationship between the DOP and the rate of degradation can be seen in Figure 4.11. The degradation rate for

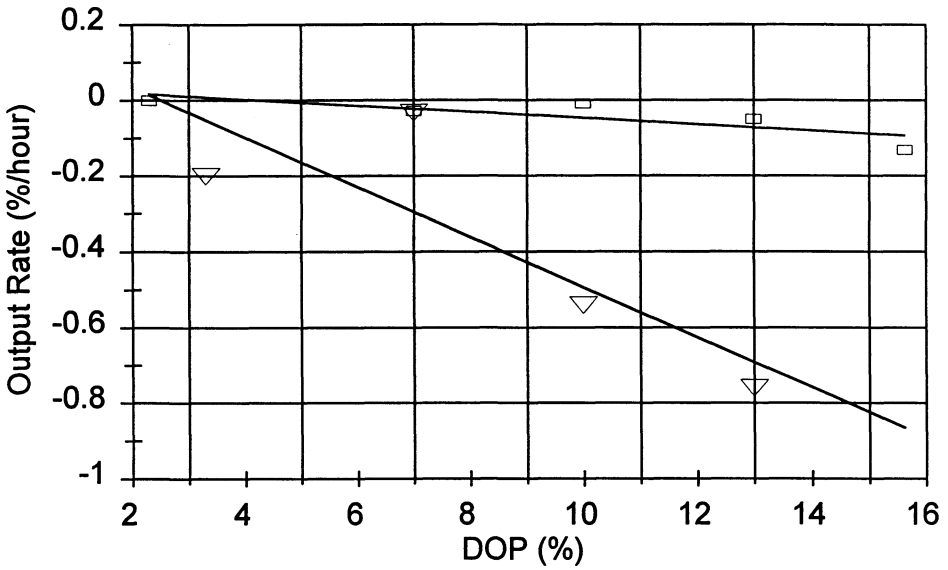

Figure 4.11 Relation between output power rate and DOP in n-region for lasers from batch D462502 for repetition rates of 1 kHz (squares) and 5 kHz (triangles).

the chip driven at a 5 kHz repetition rate was higher for the same amount of stress as for the chip driven at a 1 kHz repetition rate. A least squares fit was performed on both sets of data, and the linear correlation coefficient, |r|, was calculated to be 0.83 for the 1 kHz data set, and 0.82 for the 5 kHz data set. The probability of obtaining a larger value of |r| from a random set of data was less than 10% for the 1 kHz plot and approximately 15% for the 1 kHz plot, indicating that a linear approximation of the data is reasonable. The sensitivity to strain of normalized power for the lasers was calculated to be $-(8 \pm 3) \times 10^{-5}$ / %DOP · hour for the 1 kHz repetition rate and $-(7\pm3) \times 10^{-4}$ / %DOP · hour for the 5 kHz repetition rate. It is important to note that the DOP measurements were obtained

from the photoluminescence of the lasers with no current driving them. It is assumed that the different driving currents affect the stress in the laser as well.

The limit of stress tolerance of the D462502 batch lasers was calculated using the linear fitted functions. The functions were solved for a DOP value in the n-region that would correspond to a degradation rate of 0.25 %/hour, which would yield an approximate degradation of 25% at 100 hours. For the repetition rate of 1 kHz, the limit was found to be 35 ± 1 %. For the repetition rate of 5 kHz, the limit was found to be 6.30 ± 0.04 %. Comparison of the values revealed that the tolerance is related to the frequency of current pulses.

Degree of polarization was also measured for chips from the poor batch QX173B. A summary of DOP measurements is presented in Table 4.2. Again, for a given applied force, tensile and compressive stresses were approximately equal in magnitude in the p- and n-regions, respectively, and stresses in the active layer calculated with experimental results showed similar values as simply-supported beam approximation. DOP images of the output facet of chips with 0.4 N and 2.5 N applied force are shown in Figure 4.12 (a) and Figure 4.12 (b), respectively. The same applied force to chips from the poor batches produced approximately the same DOP values as the reliable chips, but the performance was inferior. This suggests that any defects which may have been present in the laser

Force (N)	Calculated σ_{xx} ($\times 10^8$ dyn/cm^2)	Active Layer		n-side	
		DOP (%)	σ_{xx} ($\times 10^8$ dyn/cm^2)	DOP (%)	σ_{xx} ($\times 10^8$ dyn/cm^2)
0	0	-1.1 ± 0.3	2.2 ± 0.6	1.1 ± 0.2	-2.2 ± 0.4
0.4	3.3	-2.9 ± 0.5	6 ± 1	2.7 ± 0.4	-5.3 ± 0.8
0.9	7.4	-5.1 ± 0.9	10 ± 2	5.3 ± 0.7	-10 ± 2
1.4	17	-7 ± 1	14 ± 2	7 ± 1	-14 ± 2
2.5	21	-11 ±1	22 ± 2	11 ± 2	-22 ± 4

Table 4.2 Stress measurements for QX173A laser chip under various forces.

material may have penetrated throughout the device when strain was introduced into the material, thus reducing the useful lifetime of the laser.

The DOP patterns arising from the strain induced by the probe were similar to the patterns observed at the output facet of a GaAs-based laser chip bonded to a heat sink. By applying force with the probe to a chip from a desired batch, one can approximate how much a laser would degrade with a certain amount of bonding stress. Thus, the method described in this experiment can be a tool to test the stress tolerance of lasers and to characterize lasers before they are bonded and life tested.

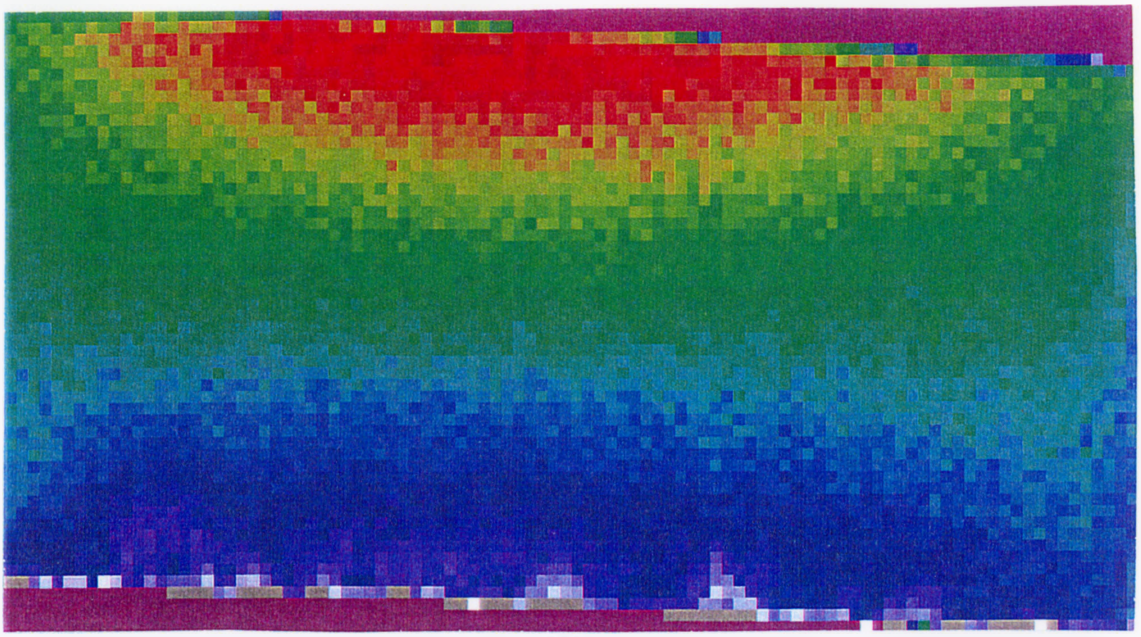

(a)

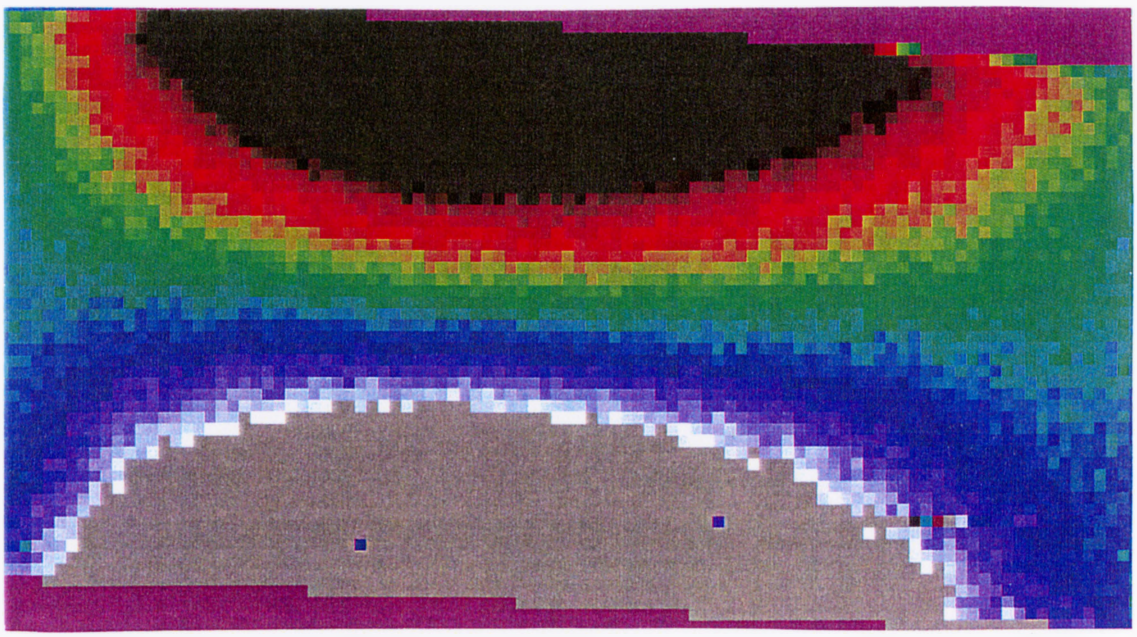

(b)

Figure 4.12 DOP images of unbonded GaAs-based lasers from batch QX173B with (a) 0.4 N and (b) 2.5 N applied forces.

4.4 Summary

In this study of high power GaAs-based lasers, it has been observed that the reliability of such lasers can be affected by the amount of force applied to the chip. Results have shown that, as the applied force increased on a chip centred on a groove, the rate of degradation in the output power increased. For standard lasers, stress sensitivity to the normalized power was found to be - $(8 \pm 3) \times 10^{-5}$ / %DOP · hour for the 1 kHz repetition rate and - $(7 \pm 3) \times 10^{-4}$ / %DOP · hour for the 5 kHz repetition rate for standard GaAs-based lasers. For the lasers studied in this work, a limit of stress tolerance in the n-region of 35 ± 1 % and 6.30 ± 0.04 % for 1 kHz and 5 kHz repetition rate, respectively, was determined such that DOP values beyond these would lead to failed performance, as defined by EG&G requirements, over a life test of approximately 100 hours.

Chapter 5 Conclusion

As with many semiconductor devices, the reliability of high-power GaAs-based lasers is an important issue for the demands of modern applications. Many aspects must be investigated to ensure reliable performance. Stress caused by the packaging of GaAs-based lasers has been an important aspect studied in this work. In addition to this, the direct result of applied stress on the lifetime of these lasers has been observed.

Life testing and bonding stress were studied on lasers using different bonding materials. Life test results have shown a low life expectancy for the lasers bonded to OFHC Cu heat sinks using Ablebond conductive epoxy. The type of adhesive as well as the heat sink affect the bonding stress and performance of the laser. Bonding stress, as measured by the degree of polarization, was lowest in the lasers when the heat sink and adhesive had coefficients of thermal expansion closely matched to the CTE of the laser material. In addition, physical aspects, such as adhesive distribution and voids, of the bonding adhesives were studied to obtain further insight into effects on bonding stress. Results suggest that the effects of the bonding adhesive on reliability should be considered in the design of chip packaging.

The reliability of lasers can be affected by the amount of force applied to the chip. In this study, results have shown that within experimental precision, as the applied force increased on a chip centred on a groove, the rate of degradation in the output power increased linearly. Stress sensitivity to the normalized power was found to be - $(8 \pm 3) \times 10^{-5}$ / %DOP · hour for the 1kHz repetition rate and - $(7 \pm 3) \times 10^{-4}$ / %DOP · hour for the 5kHz repetition rate for standard GaAs-based lasers. For the lasers studied in this work, a stress tolerance in the n-region of 35 ± 1 % and 6.30 ± 0.04 % for 1 kHz and 5 kHz repetition rate, respectively, was determined such that, DOP values beyond these would lead to failed performance, as defined by EG&G requirements, over a life test of approximately 100 hours. As well, the performance of lasers selected from a poor batch degraded at an accelerated rate after several hours of operation.

Experiments performed for this thesis have had significant impacts on research of semiconductor lasers. Bonding stress data, as measured by degree of polarization, have been important for reliability studies at EG&G Optoelectronics. Measurements of output power with different applied forces have demonstrated a useful method to monitor lasers and to characterize batches before they are packaged and life tested. The contributions of this thesis suggest efficient methods of the packaging and testing of semiconductor diode lasers.

Chapter 6 Future Work

6.1 Introduction

The experiments performed for this project have provided useful information into the effects of packaging on diode lasers. Results obtained in this work have shown that the process of packaging is not trivial, and that the heat sink and the bonding adhesive must be chosen carefully to ensure reliability in lasers. As well, the lifetime of lasers has been shown to depend on the amount of stresses induced in the devices.

The data obtained for this project have been achieved through the analysis of the degree of polarization of photoluminescence. The technique of studying polarization resolved measurements has a spatial resolution of approximately 1 μm and a strain resolution of 10^{-5}, which allow for measurements that provide detailed stress patterns over large areas of a semiconductor, such as the front facet of a diode laser. As well, scans of such samples containing about 10,000 data points can be obtained in less than 2 hours. Repeatability of measurements is possible because of the relatively non-destructive aspect of this technique. Because of these benefits, more work can be done to observe how stress is induced in packaging and the processing of diode laser, and how strain affects the performance of such devices.

6.2 Further Research

The effects of bonding a laser to a heat sink were investigated in this project. However, the effects of wire-bonding were not observed. Thermal stresses caused by top bonding may become significant if high temperatures are required. If the laser is mounted active-up, heating caused by current injection may be an issue if the wire bond is placed too close to the stripe. The effects of wire bonding can also affect the laser lifetime. To minimize strain, the wire-bonding, heat sink and bonding adhesive may be selected so that they are thermally matched with the laser material.

Research into the effect of strain on the reliability of lasers requires more investigation. Degree of polarization measurements obtained from the photoluminescence at the front facet of lasers do not provide information about the stress within the entire device. Thus, 'three-dimensional' DOP analysis can be a method to analyze the propagation of stress within a laser. One possible experiment would be to etch or polish layers from a laser, and perform DOP measurements at various stages of etching. Such a procedure would be similar to the experiment reported for this project which studied the distribution of stress within the active layer of a laser. From this procedure, however, information about possible defects or sources of failure may be discovered. Information from this experiment would be helpful in revealing failure mechanisms.

As was mentioned in this project, the strain in a laser may be altered with different levels of current running through the device. To observe the effects of injected current on the strain in the active layer, DOP measurements may be obtained at the front facet while operating a laser at various current levels. Studies of lasers before and after life testing could also give insight into changes in stress that occur as a result of life testing.

In addition to the effects of bonding stress, stress induced by different stages of processing can be investigated. It has been observed in this work that the unbonded lasers processed at EG&G had noticeable strain, possibly caused by metallization. The effects of dielectric and metal layers can be investigated such that the strain introduced by these steps can be minimized.

6.3 Summary

Studies of mechanical stress in semiconductor-based lasers are still relatively new and require more investigation. The benefits such as strain and spatial resolution offered by degree of polarization measurements are appropriate for further research of semiconductor devices such as lasers.

Chapter 7 References

1. M. Fukuda, M. Okayasu, J. Temmyo and J. Nakano, 'Degradation behavior of 0.98-μm strained quantum well InGaAs/AlgaAs lasers under high-power operation', *IEEE Journal of Quantum Electronics*, **30**, 471-476 (1994).

2. S.-L. Chaung, A. Ishibashi, S. Kijima, N. Nakayama, M. Ukita and S. Taniguchi, 'Kinetic model for degradation of light-emitting diodes', *IEEE Journal of Quantum Electronics*, **33**, 970-979 (1997).

3. C. S. Adams, and D. T. Cassidy, 'Effects of stress on threshold, wavelength, and polarization of the output of InGaAsP semiconductor diode lasers', *Journal of Applied Physics*, **64**, 6631-6638 (1988).

4. A. Jakubowicz, 'Material and fabrication-related limitations to high-power operation of GaAs/AlGaAs and InGaAs/AlGaAs laser diodes', *Materials Science and Engineering*, **B44**, 359-363 (1997).

5. O. Ueda, 'Materials-related reliability aspects of III-V optical devices', *Materials Science and Engineering*, **B20**, 9-20 (1993).

6. N. Wada, S. Sakai, S. Yoshimi, Y. Shintani and M. Fukui, 'GaAs/AlGaAs light emitters fabricated on undercut GaAs on Si', *Japanese Journal of Applied Physics (Part 1)*, **33**, 1268-1274 (1994).

7. P. G. Eliseev and A. V. Khaidarov, 'Role of mechanical stresses in gradual degradation of light-emitting diodes and injection lasers', *Soviet Journal of Quantum Electronics*, **5**, 73-74 (1975).

8. P. D. Colbourne and D. T. Cassidy, 'Imaging of stresses in GaAs diode lasers using polarization-resolved photoluminescence', *IEEE Journal of Quantum Electronics*, **29**, 62-68 (1993).

9. B. Wakefield, 'Strain-enhanced luminescence degradation in GaAs/GaAlAs double-heterostructure lasers revealed by photoluminescence', *Journal of Applied Physics*, **50**, 7914-7916 (1979).

10. L. Krishan, S. Niranjana, N. Goswami, J. Wurfl, H. L. Harnagel, 'Effect of metallization on crystalline perfection and level of stress in semi-insulating and n-type gallium arsenide single crystal wafers', *Journal of Applied Physics*, **67**, 4105-4133 (1990).

11. J. Yang, and D. T. Cassidy, 'Strain measurement and estimation of photoelastic effects and strain-induced optical gain change in ridge waveguide lasers', *Journal of Applied Physics*, **77**, 3382-3387 (1995).

12. P. D. Colbourne and D. T. Cassidy, 'Dislocation detection using polarization-resolved photoluminescence', *Canadian Journal of Physics*, **70**, 803-812 (1992).

13. C. Li, Z. Mai, S. Cui, J. Zhou, A. Ding, 'Determination of stress in GaAs/Si material', *Journal of Applied Physics*, **66**, 4767-4769 (1989).

14. R. L. Hartman, and A. R. Hartman, 'Strain-induced degradation of GaAs injection lasers', *Applied Physics Letters*, **23**, 187-196 (YEAR).

15. J. W. Tomm, R. Muller, A. Barwolff, M. Neuner, T. Elsaesser, D. Lorenzen, F. X. Daiminger, A. Gerhardt and J. Donecker, 'Direct spectroscopic measurement of packaging-induced strains in high power laser diode arrays', in Conference on Testing, Packaging, and Reliability of Semiconductor Lasers IV, **3626**, 138-147 (1999).

16. K. Suzuki, O. Suzuki and M. Komagata, 'Conductive adhesive materials for lead solder erplacement', *IEEE Transaction on Components, Packaging, and Manufacturing Technology - Part A*, **21**, 252-258 (1998).

17. S. K. Kang, R. S. Rai, and S. Purushothaman, 'Development of high conductivity lead (Pb)-free conducting adhesives', *IEEE Transaction on Components, Packaging, and Manufacturing Technology - Part A*, **21**, 18-22 (1998).

18. P. Savolainen and J. Kivilahti, 'A solder ally filled z-axis conductive epoxy adhesive', Journal of Adhesion, **49**, 187-196 (1995).

19. G. E. Pikus and G. L. Bir, 'Effect of deformation on the hole energy spectrum of germanium and silicon', *Soviet Physics Solid State*, **1**, 1502-1517 (1960).

20. P. D. Colbourne, Measurement of Stress in III-V Semiconductors Using the Degree of Polarization of Luminescence (Ph.D. Thesis), McMaster University, Hamilton, Ontario, 1992.

21. S. W. Corzine, R.-H. Yan, L. A. Coldren, 'Optical gain in III-V bulk and quantum well semiconductors', in Quantum Well Lasers, Academic Press, Inc., San Diego, 1993, pp. 17-96.

22. R. L. Liboff, Introductory quantum mechanics, Holden-Day, Oakland, 1980.

23. D. R. Lide, ed., CRC Handbook of Chemistry and Physics, 71st ed., CRC Press, Boca Raton, Fla., 1990, p.12-107.

24. J. R. Davis, Metals Handbook, 2nd ed., ASM International, Materials Park, OH, 1998, p. 667.

25. A. H. Moore and S. Meszaros. (Unpublished).

26. J. Yang, Title (PhD. Thesis), McMaster University, Hamilton, Ontario, 1994.

27. R. A. Johnson, Miller and Freund's Probability and Statistics for Engineers, 5th ed., Prentice Hall, Englewood Cliffs, NJ, 1994, pp.315-318.

28. M. E. Straumanis, J.-P. Krumme and M. Rubenstein, 'Article', *Journal of the Electrochemical Society*, **114**, 640 (1967).

29. D. R. Lide, ed., CRC Handbook of Chemistry and Physics, 71st ed., CRC Press, Boca Raton, Fla., 1990, p.15-33.

30. X. Luo and D. D. L. Chung, 'A comparative study of silver-epoxy and tin-lead solder in their joints with copper, through mechanical and electrical measurements during debonding', *Journal of Materials Science*, **34**, 273-281 (1999).

31. Ablestik, Ablebond 84-1 LMINB1 Epoxy product specifications, 1997.

32. A. I. Technology, Inc., Prima Bond ME 8412 Epoxy product specifications, 1994.

33. R. Juvinall, Fundamentals of Machine Component Design, Wiley, New York, 1983.